

Alma Mater Studiorum – Università di Bologna

DOTTORATO DI RICERCA IN  
SCIENZE BIOMEDICHE E NEUROMOTORIE

Ciclo XXXIII

**Settore Concorsuale: 05/D1**

**Settore Scientifico Disciplinare: BIO/09**

CDKL5 DEFICIENCY DISORDER: THE POTENTIAL OF A GABA<sub>B</sub> RECEPTOR  
ANTAGONIST TO RESCUE FUNCTIONAL AND STRUCTURAL  
IMPAIRMENTS IN THE PERIRHINAL CORTEX OF A MOUSE MODEL

**Presentata da:** Anna Cecilia Berardi

**Coordinatore Dottorato**

Prof. Matilde Yung Follo

**Supervisore**

Prof. Giorgio Aicardi

**Co-Supervisore**

Prof.ssa Elisabetta Ciani

**Esame finale anno 2021**

## ABSTRACT

CDKL5 (cyclin-dependent kinase-like 5) deficiency disorder (CDD) is a severe neurodevelopmental encephalopathy characterized by early-onset epilepsy and intellectual disability. Studies in mouse models have linked CDKL5 deficiency to defects in neuronal maturation and synaptic plasticity, and disruption of the excitatory/inhibitory balance. Interestingly, increased density of both GABAergic synaptic terminals and parvalbumin inhibitory interneurons was recently observed in the primary visual cortex of Cdkl5 knockout (KO) mice, suggesting that excessive GABAergic transmission might contribute to the visual deficits characteristic of CDD. However, the functional relevance of cortical GABAergic circuits abnormalities in these mutant mice has not been investigated so far. Here we examined GABAergic circuits in the perirhinal cortex (PRC) of Cdkl5 KO mice, where we previously observed impaired long-term potentiation (LTP) associated with deficits in novel object recognition (NOR) memory. We found a higher number of GABAergic (VGAT)-immunopositive terminals in the PRC of Cdkl5 KO compared to wild-type mice, suggesting that increased inhibitory transmission might contribute to LTP impairment. Interestingly, while exposure of PRC slices to the GABA<sub>A</sub> receptor antagonist picrotoxin had no positive effects on LTP in Cdkl5 KO mice, the selective GABA<sub>B</sub> receptor antagonist CGP55845 restored LTP magnitude, suggesting that exaggerated GABA<sub>B</sub> receptor-mediated inhibition contributes to LTP impairment in mutants. Moreover, acute *in vivo* treatment with CGP55845 increased the number of PSD95 positive puncta as well as density and maturation of dendritic spines in PRC, and restored NOR memory in Cdkl5 KO mice. The present data show the efficacy of limiting excessive GABA<sub>B</sub> receptor-mediated signaling in improving synaptic plasticity and cognition in CDD mice.

## **INDEX**

- Introduction page 4
  
- Materials and Methods page 20
  
- Results page 30
  
- Discussion page 45
  
- References page 49

## INTRODUCTION

CDKL5 (Cyclin-dependent kinase-like 5) deficiency disorder is a neurodegenerative disease characterized by early episodes of epileptic seizures, severe neurological disability, stereotyped hand movements, motor stiffness and language difficulties. Various dysmorphic features have also been described in individuals with a CDKL5 mutation including large deep-set eyes, strabismus, high forehead, full lips, wide mouth and widely spaced teeth. The presence of typical facial or other features could provide additional assistance in the clinical identification of individuals with a CDKL5 mutation (Fehr et al., 2013).

This pathology is related to the occurrence of mutations in the X chromosome of the CDKL5 gene. This gene is located on the short arm of the X chromosome at position 22 (Xp22) and encodes for a widely expressed serine / threonine kinase in the brain (Zhou et al, 2019). To date, more than 500 genes have been identified in the human genome that code for kinases (Manning et al., 2002); however, many of them have not yet been characterized and their functions remain unknown.

The kinase encoded by the CDKL5 gene was discovered in 1998 (Montini et al., 1998), but its function was partially elucidated only recently when it was implicated in neurological disorders. In fact, mutations affecting the X chromosome of the CDKL5 gene lead to disorders characterized by symptoms (epileptic attacks, severe neurological disability, autistic traits, motor dysfunctions) also present in X-linked Infantile Spasm Syndrome (ISSX), Rett syndrome (RTT), Angelman syndrome and Autism. These neurological symptoms led to some hypotheses about the role of the CDKL5 gene in brain development and function. Since the association of mutations with neurological disorders has been highlighted, numerous studies have been undertaken aimed at clarifying the role(s) and function(s) of the gene.

***Discovery and evolution of CDKL5 encephalopathy***

The CDKL5 gene is abundantly expressed in the human and murine brain. The gene was first identified in 1998 (Montini et al., 1998) through a cloning study which identified diseased genes present in the Xp22 region. The CDKL5 deficiency disorder, sharing many common features with RTT, was initially referred to as the "Hanefeld variant" of RTT.

RTT (Guerrini and Parrini, 2012) is a pathology which occurs in childhood; it is characterized by a failure to grow up, regression of language and hand use, significant neurocognitive damage and autistic traits. This pathology occurs in females (it is not compatible with life in males) with an incidence of 1: 10,000 and is attributable to mutations in the MeCP2 gene (identified in 1999), which are present in 95% of the typical form of RTT .

The diagnosis of RTT is based not only on characteristic clinical elements for identifying the typical form but also for identifying the atypical forms, where the MeCP2 is mutated in 50-70% of cases.

The main problem with these patients is represented by motor difficulties. The most evident is represented by stereotypical movements of the hands, interrupted gait, and widespread dystonia. Other motor difficulties are represented by tremors, chorea, grimacing of the face and grinding of the teeth. Another problem is the impairment of gastrointestinal functions such as the ability to chew and swallow, gastroesophageal reflux, and severe constipation. Breathing difficulties such as hyperventilation and prolonged pauses in breathing sometimes occur which result in cyanosis and even loss of consciousness. Seizures usually occur and are related to the severity of the phenotype. However, the brains of patients affected by RTT do not show major changes such as neuronal atrophy, demyelination and degeneration, indicating that RTT is not a neurodegenerative disease. There is a decrease in brain volume and in the number of neurons in certain areas such as hippocampus, cerebral cortex, and hypothalamus. The size and dendritic arborization are decreased in the neurons of the pyramidal cortex, as well as the density of the spines in the neurons of the frontal cortex and in the CA1 of the hippocampus (Katz et al., 2012). To date, there are no effective treatments for RTT.

Mutations in genes such as CDKL5 or FOXP1 give rise to phenotypes that can be superimposed on RTT and for a long time they were defined as “variants of RTT”. Today they are defined as pathologies in themselves. The first description of CDKL5 mutations dates to 2003 thanks to the *Kalscheuer* study in which 2 girls with infantile spasms and profound developmental delay were diagnosed. In this study a "breakpoint" was found at the gene level. Subsequently other researchers studied the gene in patients diagnosed with RTT but who were negative on the MeCP2 test. The study ended with the identification of mutations in the CDKL5 gene in patients with early epilepsy episodes (Tao et al., 2004; Weaving et al. al., 2004; Scala et al., 2005; Bahi-Buisson et al., 2008).

In recent years, as a result of patients' clinical data, a phenotypic spectrum has been outlined that goes from milder forms, characterized by the possibility of walking independently and lighter forms of epilepsy, to more severe forms with uncontrollable epilepsies, severe microcephaly and lack of normal development parameters (Guerrini and Parrini, 2012). Unlike RTT, children with CDKL5 mutations do not show regression, or even impaired autonomic functions, and a typical gaze. The lowest common denominator of encephalopathy is characterized by early seizures within 5 months, severe developmental delay, head growth retardation, difficulty in communicating and stereotyped hand movements (Melani et al., 2011). Babies are usually normal at birth and only later show developmental difficulties: no ability to move hands, no eye contact, difficulty in communicating, developmental delay. Only about 1/3rd of them are able to walk. An important problem is represented by respiratory problems (tachypnea, dyspnea) and poor rest efficiency. Sometimes gastrointestinal problems, hypotonia and scoliosis develop. A common feature is seizures that manifest as infantile spasms with an onset between 5 days and 4 months of life. The epileptic pattern is characterized by clinical tonic seizures then mutating into myoclonuses repeated at the distal level. Remission of epileptic seizures occurs in about 1/3rd of patients as they get older. The rest continue to show uncontrollable spasms associated with multifocal and myoclonic seizures.

### *The protein CDKL5*

The highest expression of CDKL5 mRNA is found in the brain, but is also elevated in other tissues such as the testes, placenta, uterus, spleen, and lungs, while it is low in the heart, kidneys, skeletal muscle and in the liver. The expression of CDKL5 changes according to the stage of development in the rodent brain; it has low levels at the embryonic level, while its expression is enhanced immediately after birth (stage p14 in mice) and then remains constant in adults. The fact that its expression is induced immediately after birth suggests a role in neuronal maturation (Rusconi et al., 2008). In the mouse brain, CDKL5 is mainly expressed in the frontal lobe, hippocampus, thalamus, striatum, and olfactory bulb. Among these areas, the frontal lobe and the hippocampus are important for cognitive functions and memory, while the striatum is involved in voluntary movements. The alteration of the functions of these areas leads to the symptoms observed in CDKL5 patients.

In the cerebral cortex, the highest levels of mRNA expression were found in the motor cortex, cingulate cortex, piriform cortex and entorhinal cortex. In the hippocampus, high levels of CDKL5 mRNA were found in Cornu Ammonis, but not in the dentate gyrus; this may be due to the fact that mRNA transcription takes place in completely mature neuronal phenotypes, and the dentate gyrus is characterized by neurogenesis in adulthood. Instead, a low expression was found in dopaminergic areas such as the substantia nigra and the ventral tegmental area, and in noradrenergic areas such as the locus coeruleus (Kilstrup-Nielsen et al., 2012).

CDKL5 is a nuclear and cytoplasmic protein; the nuclear fraction increases with brain development (starting from stage P14 in mice) and there is a different distribution between the two compartments depending on the brain area analyzed. For example, in the cerebellum more than 80% of CDKL5 remains in the cytoplasm, while in the cortex it is equally distributed. The exchange between the two compartments takes place through shuttles that provide for an active transport involving the C-terminal portion and the nuclear receptor CRM1; this transport is regulated by various stimuli including glutamate. Accumulation in the cytoplasm is also a consequence of the activation of the ex-

trasynaptic NMDA receptors. These receptors play a role in synaptic plasticity and in the phosphorylation of the transcription factor CREB, suggesting how their anomaly can lead to epileptic seizures.

### ***Structure of the protein CDKL5***

Kinases are enzymes that modify the activity of other proteins by adding phosphate groups in specific positions; in this way they mediate most of the translation signals in eukaryotic cells and control many cellular processes including metabolism, transcription, cell cycle progression, apoptosis, and differentiation. In the brain, these enzymes are important signal transducers involved in neuronal development and function. The kinase family in eukaryotes represent a large family of homologous proteins characterized by the presence of a highly conserved domain of 250-300 aa. This family is divided into serine-threonine kinases and tyrosine kinases. The CDKL5 was initially defined as STK9 by Montini et al. (1988) for homology with the latter. Later it assumed its current name given the homology with cell division kinases-like (CDKL). The CDKL5 gene occupies 240 kb and is composed of 24 exons of which the first 3 (1, 1a, 1b) are not translated, while the coding sequence is contained between exons 2-21. The CDKL5 protein belongs to the CMGC serine-threonine kinase family, which includes: cyclin-dependent kinases (CDKs), mitogen-activated protein kinases (MAP kinases), glycogen synthase kinases (GSKs), and CDK-like (CDKL) kinases. This protein is characterized by an N-terminal catalytic domain (aa 13-297) and a long C-terminal domain that regulates the catalytic activity, subcellular localization and stability of the protein (Rusconi et al., 2008). The N-terminal domain (catalytic domain) contains the ATP binding region (aa 14-47) and the kinase activation site (aa 131-143).

The degradation of this protein occurs through proteases and this programmed death is functional to the correct brain development. In this regard, in fact, it has been shown that a depolarization leads to an increase in CDKL5 levels; this induction is prolonged in young neurons, while in mature

neurons the stimulation of NMDA receptors stimulates the protein responsible for the dephosphorylation of CDKL5 followed by proteolytic degradation (La Montanara et al., 2015). The activity of CDKL5 is carefully regulated and posttranslational modification is the most important mechanism that regulates the activity of a protein.

CDKL5 autophosphorylates itself and it is present in this form in cells (La Montanara et al. 2015), therefore it is possible that this is necessary for activation. It can also be phosphorylated by other proteins such as BDNF (Chen et al, 2010) in cultured neurons, but the responsible kinases *in vivo* have not yet been identified. Phosphorylation is a reversible process and dephosphorylation is induced by enzymes called phosphatases. La Montanara et al. (2015) showed that CDKL5 is dephosphorylated by PP1 and is activated by neuronal activity. This process is mediated by NMDA receptors.

To date, about 200 cases of CDKL5 encephalopathy have been described (Fehr et., 2013) and these data have been used to study mutations in the gene and, where possible, to identify a correlation between genotype and phenotype.

The most important domains characterized by the mutations are: ATP-binding domain (aa 14-47), the activation site (aa 127-144) and a terminal COOH portion of about 700 aa.

Missense mutations are almost exclusively localized in the C-terminal and result in loss of kinase activity leading to more severe cases of encephalopathy, suggesting that enzyme activity is essential for normal neurological development (Bahi-Buisson et al., 2008).

Conversely, patients with ATP binding site mutations walk, have better use of the hands and less frequent epileptic episodes. Bahi-Buisson et al. (2008) observed how mutations in the terminal C portion lead to milder forms than those in the catalytic portion. In fact, the C-terminal portion has a regulatory role for the catalytic activity of CDKL5 and modulates the subcellular activity. A correlation between genotype and phenotype was reported by Weaving et al. (2004): two twins with the gene mutated in the same way, resulting in two different phenotypes. One twin showed a phenotype

similar to patients with RTT, the other one an autistic disorder with moderate neurological disability. This may be due to other genes modified by epigenetic or environmental factors.

### ***CDKL5 functions***

CDKL5 regulates neuronal migration, axonal and synaptic development and dendritic morphogenesis; the following mechanisms of action have been proposed overall.

- ***CDKL5 suppresses cell proliferation***; this was investigated in neuroblastomas (cell lines SHSY5y and SKNBE) where it was observed that the overexpression of CDKL5 induced by retinoic acid resulted in increase in neuronal differentiation, arrest of the cell cycle in the G0/G1 phase, and inhibition of cell proliferation (Valli et al., 2012). In support of this, the lack of this gene in the mouse brain increases the proliferation in the granulocytes of the dentate gyrus (Fuchs et al., 2014). Furthermore, Valli et al. (2012) showed that CDKL5 expression is inhibited by MYCN, a transcription factor that promotes cell proliferation. The mechanism of action in proliferation is still unclear, but recently CDKL5 has been localized in the centrosomes of dividing cells and has been found to be essential for a correct cell division process (Barniero et al., 2017). Since centrosomes play an important role in neuronal development, CDKL5 might turn off the proliferation through a mechanism that involves the regulation of centrosomes.
- ***CDKL5 regulates neuronal migration***; in fact, an under-expression of CDKL5 by RNAi results in a delay in the migration of layers II-III of pyramidal neurons (Chen et al., 2010; Ricciardi et al., 2012). In addition, the CDKL5 gene interacts with IQGAP1 (regulator of migration and neuronal polarity) by regulating its association with its Rac1 effectors, microtubules and the CLP1170 protein. Damaged microtubules contribute to migratory defects in neurons lacking the CDKL5 gene.

- ***CDKL5 regulates axonal growth*** by interacting, as demonstrated by the study by Nawaz et al. (2016), with the Shootin1 protein; both proteins are located in the growth cones in the early stages of neuronal development. If CDKL5 is silenced or overexpressed, neurons with multiple axons increase and this can be attributed to a dysregulation in the phosphorylation of the Shootin1 protein (Nawaz et al., 2016). If, on the other hand, the gene is under-regulated it does not prevent the formation of axons (Chen et al., 2010; Cheng and Poo, 2012; Nawaz et al., 2016). These data, obtained *in vitro* in murine neurons, suggest that CDKL5 is not decisive for the formation of axons, but exerts a modulatory action. However, these processes have not yet been investigated *in vivo*.
- ***CDKL5 regulates dendritic arborization***; the study by Chen et al. (2010) describes both the role and the mechanism of action of CDKL5 in the modulation of dendritic arborization. CDKL5 forms a protein complex with Rac1, a fundamental regulator of neuronal morphogenesis. Rac1 can also be activated by neurotropic factors such as BDNF (Zhou et al., 2007; Chen et al., 2010). If CDKL5 is downregulated, it abolishes this BDNF-mediated activation of Rac1 suggesting that the CDKL5 gene plays an essential role in BDNF-Rac1 signaling. If CDKL5 is overexpressed, the dendritic length is increases in a kinase-dependent manner (Chen et al., 2010), suggesting that CDKL5 regulates a signaling pathway that controls dendritic growth. The mechanism of CDKL5 in dendritic development has not been fully understood, but the activity of the catalytic portion seems essential (Chen et al., 2010). In fact, patients with mutations affecting these domains have more severe phenotypes of the disease. In addition, other circuits would be involved in the dendritic arborization pattern typical of CDKL5 encephalopathy, such as AKT/mTOR and AKT/GSK-3b (Wang et al., 2012; Fuchs et al., 2014), which are involved in the regulation of neuronal morphogenesis and that are damaged in neuronal disorders. Therefore, it is reasonable to assume that CDKL5 controls dendritic development by regulating multiple substrates and circuits.

### ***Role of CDKL5 in the formation and function of synapses***

Typically, an altered morphology of the spines (i.e., dendritic protrusions with excitatory synapses) is observed in patients with neurological disabilities (Purpura, 1974). This also occurs in patients with CDKL5 encephalopathy: CDKL5 is increased in post-synaptic densities (PSDs), protein agglomerates in dendritic spines involved in synaptic transmission, signal translation and neuronal adhesion (Ricciardi et al., 2012; Zhu et al., 2013). Synaptic localization suggests that CDKL5 is involved in synaptic development and function and this has been experimentally tested in several studies using RNAi and KO mice. In the study performed in murine neurons by Ricciardi et al. (2012), the downregulation of CDKL5 mediated by RNAi *in vitro* and *in vivo* led to an increase in the number of dendritic protrusions and immature spines; silencing CDKL5 led to a severe deficit in spinal morphology and density. Similar results were obtained in neurons derived from iPSCs, indicating that the CDKL5 gene is required for the formation of the correct number of spines. On the contrary, Zhu et al. (2013) observed that the downregulation of CDKL5 led to a decrease in the density and size of the spines. This difference seems to be due to the insertion time of the RNAi. In the first study it was inserted when the spines started to grow, in the “early stage”, whereas in the second one it was inserted in the “late stage”, when the spines were already formed. Therefore, it appears that the gene is required for maturation of the spines and the maintenance of the existing ones. Despite the differences in spinal morphology, the number of excitatory synapses was reduced in both studies. This is documented by reduced expression of synthetic markers and reduced excitatory post-synaptic currents (EPSC) frequency in neurons expressing CDKL5 RNAi (Ricciardi et al., 2012; Zhu et al., 2013). This suggests that CDKL5 is a key factor in regulating synapse formation and that changes in synaptic excitation strength are responsible for neurological symptoms. The effect of CKL5 deficiency disorder on spine development was examined in KO mice leading to conflicting results. On one hand there is a reduction in spine density and in the number of mature spines

in DG granule cells, in pyramidal hippocampal CA1 neurons, and in cortical neurons (Della Sala et al., 2016; Trazzi et al., 2018). On the other hand, the level of expression of the postsynaptic markers was reduced (Pizzo et al., 2016). However, when CDKL5 was specifically removed only from frontal excitatory neurons, there was an increase in spine density and volume, and an increase in the frequency of EPSC (Tang et al., 2017). This difference can be traced back to the following hypothesis: a deletion of CDKL5 genes in large groups of neurons can trigger compensatory mechanisms that make it difficult to assess the loss of phenotype in individual cells. Several studies show that correct kinase activity and targeting are required to regulate correct synaptic development by CDKL5. In excitatory synapses, CDKL5 binds to the palmitate isoform of PSD95 (protein involved in learning and memory) and this allows the CDKL5 to be directed towards the excitatory postsynaptic sites (Zhu et al., 2013). The lack of CDKL5-PSD95 interaction leads to a lack of spinal development. In fact, this link to the postsynaptic site allows CDKL5 access to the effectors at the base and is critical for synaptic development. One of the effectors of this bond is NGL-1, which is an adhesion molecule important for synaptic formation and synaptic homeostasis. In the synapse, CDKL5 binds and phosphorylates NGL1 at the level of Serine 631 and this phosphorylation allows the interaction between NGL and PSD95, which in turn promotes the development of dendritic spines. NGL1 binds to PSD95 via the BDZ domain of the C-terminal site which is very close to Serine 631 (the CDKL5 phosphorylation site). This guarantees a stable association between PSD95 and NGL-1 (Ricciardi et al. 2012). Della Sala et al. (2016) observed that KO mice show a reduction in spinal density with a reduction of the puncta at the level of PSD95. In addition to NGL1, there may be other effectors and circuits that mediate the synaptic function of CDKL5. In fact, in the case of CDKL5 encephalopathy the restoration of the spinal pattern is incomplete if a phosphomimetic NGL-1 is used.

### ***Role of CDKL5 in maintaining synaptic function***

CDKL5 continues to be expressed, even in adulthood, suggesting that it plays a role not only in neuronal development, but also beyond. Indeed, mature spine stabilization and LTP are impaired in adult mice with CDKL5 encephalopathy (Della Sala et al., 2016) and they have impaired hippocampus-dependent memory (Wang et al., 2012; Tang et al., 2017). To date, little is known about the role in maintaining synaptic function and structure; however, the gene seems important in ensuring correct synaptic maturation (Okuda et al., 2017).

### ***Substrates of CDKL5 at the nuclear level***

CDKL5 and MeCP2 genes are extensively co-expressed in the brain, and both of them are activated during synaptogenesis and neuronal maturation (Mari et al., 2005; Rusconi et al., 2008). *In vitro*, CDKL5 mildly phosphorylates MeCP2 (Mari et al., 2005; Kameshita et al., 2008), but *in vivo* this has not yet been tested. Moreover, it is not certain that MeCP2 is the endogenous substrate. In comparison, the phosphorylation of Dnmt 1 (the enzyme that methylates DNA at the level of CpG dinucleotides) by CDKL5 seems more efficient *in vitro* (Kameshita et al., 2008), but also in this case it is not certain that this process occurs *in vivo*. In the study by Trazzi et al. (2016) in SHSY5Y cell lines, exogenous CDKL5 phosphorylates HDAC4, a transcriptional repressor of gene expression. This phosphorylation occurs at the level of the 632 series, which regulates its subcellular localization. However, HDAC4 phosphorylation is only reduced by 25% in CDKL5 KO mice, indicating that other kinases are involved in this process.

### ***Substrates of CDKL5 at the cytoplasmic level***

NGL1 (netrin-G1 ligand) is a synaptic protein that promotes synaptic formation and maturation. In the excitatory synapses, NGL1 is localized with CDKL5 and forms a protein complex with CDKL5 and PSD95. Ricciardi et al. (2012) showed that the CDKL5 protein phosphorylates NGL1 at the level of serine 631, and that this allows its binding with PSD95 which favors synaptic development.

Another cytoplasmic substrate is represented by Amph1 (Sekiguchi et al., 2013), a protein involved in neuronal development and transmission located on the cytoplasmic side of synaptic transports. The phosphorylation of this substrate by CDKL5 (this phosphorylation occurs at the level of Serine 293; it is hampered if mutations occur in the catalytic portion of CDKL5) is even more efficient than the phosphorylation of Dnmt1, suggesting that it is more likely an endogenous substrate. This suggests a potential role of CDKL5 in the control of endocytotic processes in neurons. Furthermore, a deficiency of Amph1 has been associated with the onset of epileptic seizures and learning deficits, making it a possible candidate in the pathogenesis of CDKL5 encephalopathy. However, both of these cytoplasmic substrates have not been tested *in vivo* in KO mice.

### ***Murine models and therapeutic approaches***

To better investigate this pathology and test therapeutic approaches, murine models were generated (Wang et al., 2012; Amendola et al., 2014; Jhang et al., 2017; Tang et al., 2017; Okuda et al., 2018). These mice present various neuroanatomical anomalies and deficits in behavior including impaired learning and memory, locomotor difficulties, abnormal closure of the hind limbs, hypoactivity and irregular eye movements.

The prototype of KO mouse used in our laboratory is the model of Amendola et al. (2014), obtained through the deletion of exon 4 at the level of the allele of the CDKL5 gene. This mouse has no difference in body and brain weight compared to its wild-type counterpart and does not have spontaneous epileptic seizures. It has an abnormal closure of the lower limbs and a reduced mobility if left in a cage, but this does not happen in open spaces. Loss of CDKL5 impairs memory and learning;

this is evident in the Morris Water Maze test. A reduction in dendritic arborization was observed in the cortical layer V and in the pyramidal and hippocampal CA1 neurons. The total length of the dendrites was significantly reduced in homozygous KO mice compared to wild type (whereas in heterozygous mice this reduction was not homogeneously distributed). Moreover, there is a reduction of the cortical and hippocampal thickness of the CA1, of the striatum and of the dentate gyrus (Amendola et al., 2014). The latter was specifically investigated by Fuchs et. al. (2014) in our laboratory, who observed a high proportion of proliferating neuronal precursors (KO # WT); however, they also found an increase in apoptosis in the precursors of granule cells, resulting in a decrease in the total number of granule cells. Furthermore, the granule cells showed an immature dendritic pattern. Della Sala et al. (2016) observed that CDKL5 KO mice show a reduction in spinal density and in the amount of PSD95, a damaged LTP and a reduced frequency of EPSC.

The similarity between CDKL5 and MeCP2 encephalopathies led to the analysis of the molecular basis that could imply similarities between the two pathologies. Both genes are widely expressed in the brain and are activated during neuronal maturation and synaptogenesis (Mari et al. 2005; Rusconi et al. 2008). In addition, *in vitro* experiments have shown that CDKL5 binds and phosphorylates MeCP2, while MeCP2 regulates the gene expression of CDKL5 (Berating et al. 2006; Carouge et al. 2010; Mari et al. 2005). KO mouse models for the two encephalopathies show that a reduction in phosphorylation of rpS6 and AkT occurs, suggesting that this may be a common deficit in both pathologies. However, the different cellular distribution of the two proteins suggests that they can act through different mechanisms on common targets (Amendola et al, 2014). Therefore, the similarities between the two pathologies could derive from common defects, whereas the differences would lead to the peculiar clinical picture of the CDKL5 encephalopathy.

At the moment no cure is available for this disorder. The only available therapies are aimed at containing epileptic seizures (Bahi-Buisson and Bienvenu 2012). Recent studies have tried to identify suitable molecular targets for potential pharmacological treatments.

The GSK kinase is an inhibitory regulator of many neurological processes, whose activity is increased in case of CDKL5 deficiency and impaired hippocampal development. The treatment with SB216763 (inhibitor of GSK kinase) has proved effective in restoring hippocampal development and behavioral deficits in the KO mouse (Fuchs et al., 2015). In particular, the treatment in mice (P20-P45) allowed the restoration of neuronal precursors, dendritic maturation and synaptic connection. These effects persisted one month after the end of the treatment.

The treatment with IGF1 (activator of the AKT-mTOR pathway, which is a hypofunctional cascade in neurological disorders including encephalopathy and RTT) demonstrated the activation of Serine 240-244 phosphorylation on S6 (target kinase of AKT, present in reduced quantities in CDKL5 encephalopathy), leading to a restoration of the spinal pattern and correct expression of PSD95 (Della Sala et al, 2016).

The most effective compound was TAT-CDKL5 (Trazzi et al., 2018), which involves the fusion of the CDKL5 gene with the TAT (trans-acting activator of transcription), which is a protein that can target macromolecules inside of neurons and cells. Intracerebroventricular infusions with TAT-CDKL5 restored hippocampal development, memory, and hippocampus-dependent learning in KO mice. This approach has been weighed in the light of the brilliant results obtained by infusion of TAT-MeCP2 in the RTT where for the first time this approach was used to improve a genetic pathology.

### ***Our experimental approach***

A recent study performed in our laboratory has examined for the first time synaptic function and plasticity, dendritic morphology, and signal transduction pathways in the perirhinal cortex (PRC) of the Cdk15 KO mouse model (Ren et al., 2019). PRC is an association cortex that is crucial for recognition memory (Brown and Aggleton, 2001). Being interconnected with a wide range of corti-

cal and subcortical structures and involved in various cognitive processes, PRC provides a very interesting framework for examining how CDKL5 mutation leads to deficits at the synapse, circuit, and behavioral level. It was found that long-term potentiation (LTP) and visual recognition memory were impaired in Cdkl5 KO mice, and that PRC neurons showed a reduction in dendritic length, dendritic branches, PSD-95-positive puncta, GluA2-AMPA receptor levels, and spine density and maturation. Interestingly, an *in vivo* treatment with a TrkB agonist to trigger the TrkB/PLC $\gamma$ 1 pathway rescued defective LTP, dendritic pattern, PSD-95 and GluA2-AMPA receptor levels, and restored visual recognition memory (Ren et al., 2019).

Since CDKL5 protein is expressed at high levels in inhibitory interneurons (Rusconi, 2008), the balance between excitation and inhibition is an interesting aspect to investigate in our mouse model. Recent studies have shown that a CDKL5 deficiency resulted in an increase in the inhibitory synaptic marker VGAT (Lupori, 2019; Pizzo, 2016) and in the density of parvalbumin inhibitory interneurons (Pizzo, 2016) in the primary visual cortex, suggesting an enhancement of GABAergic transmission that might contribute to the visual deficits characteristic of CDKL5 deficiency disorder. However, the relationship between GABAergic abnormalities in the cerebral cortex and the functional deficits observed in these mice had not yet been investigated.

Inhibition mediated by GABA<sub>B</sub> receptors in the PRC plays a major role in the regulation of neuronal excitability in a frequency-dependent manner (Ziakopoulos et al., 2000), and may be critical for recognition memory formation.

Thus, in the present study we examined the effect of GABAergic transmission inhibition in the PRC of Cdk15 KO mice. We found that *in vitro* exposure to a GABA<sub>B</sub> receptor antagonist rescued defective LTP in PRC slices, and acute *in vivo* treatment with the same antagonist increased the number of PSD95 positive puncta and the number and maturation of dendritic spines in PRC, and restored novel object recognition (NOR) memory.

## MATERIALS AND METHODS

The mice used in this work derive from the *Cdkl5* KO strain in the C57BL/6N background developed in (Amendola et al., 2014) and backcrossed in C57BL/6J for three generations. Hemizygous *Cdkl5* KO (-/Y) mice were produced and karyotyped as described in the Introduction (Amendola et al., 2014). Age-matched wild-type (+/Y) littermates were used for all experiments. The day of birth was designated as postnatal day (P) zero and animals with 24 h of age were considered as 1-day-old animals (P1). Mice were housed 3–5 per cage on a 12 h light/dark cycle in a temperature- (23 °C) and humidity-controlled environment with standard mouse chow and water *ad libitum*. The animals' health and comfort were controlled by the veterinary service. Animal care and handling throughout the experimental procedures were conducted in accordance with European Community Council Directive 86/609/EEC for care and use of experimental animals with protocols approved by the Italian Minister for Scientific Research (Authorization number 175/2015-PR) and by the Bologna University Bioethical Committee. All efforts were made to minimize animal suffering and to keep the number of animals used to a minimum.

### Experimental Protocol

Experiments were performed on 2-month-old *Cdkl5* +/Y and *Cdkl5* -/Y mice. Treated animals received a single intraperitoneal injection of CGP55845 (0.5 mg/kg suspended in saline, 10mL/kg), or saline only. The dosage of 0.5 mg/kg CGP55845 was chosen on the basis of previous studies (Kleschevnikov et al., 2012). Two hours after treatment mice were behaviorally tested and subsequently sacrificed for histological analyses.

### Electrophysiology

Mice were deeply anesthetized with isoflurane before decapitation. The brain was quickly removed and immersed in ice-cold artificial cerebrospinal fluid (aCSF) composed of (in mM): NaCl, 124; KCl, 4.4; NaHCO<sub>3</sub>, 26.2; NaH<sub>2</sub>PO<sub>4</sub>, 1; CaCl<sub>2</sub>, 2.5; MgCl<sub>2</sub>, 1.3; d-glucose, 10; L-ascorbic acid, 2; continuously gassed with 95% O<sub>2</sub> - 5% CO<sub>2</sub> and adjusted for pH 7.4. Horizontal brain slices (400 µm-thick), including the PRC, the entorhinal cortex, and the hippocampus were obtained from each hemisphere using a vibrating microtome. Once obtained, the slices were left to recover for at least 60 min at room temperature in aCSF saturated with 95% O<sub>2</sub> - 5% CO<sub>2</sub>, and then stored in the same solution until usage (Aicardi et al., 2004).

*Electrophysiological recordings.* After the recovery period, a single slice was transferred to a submersion recording chamber and perfused at the rate of 3 ml/min with aCSF maintained at  $32 \pm 0.2^\circ\text{C}$  and saturated with 95% O<sub>2</sub> - 5% CO<sub>2</sub>. Recordings started 30 min after the slice was placed into the chamber. Extracellular recording electrodes consisted of borosilicate glass capillaries filled with aCSF (2–8 MΩ); stimulating electrodes were concentric bipolar electrodes (70–80 kΩ). The recording electrode was placed in layer II–III of the PRC, close to the rhinal sulcus and connected to a DC amplifier by an Ag/AgCl electrode. The stimulating electrode was inserted into the superficial layers (II–III) of the PRC at 400-500 µm from the recording electrode, in the rostral direction (temporal side of the rhinal fissure). Constant-current square pulses (0.2 ms, 20–220 µA, 0.033 Hz) were applied using a stimulus generator (Master 8, AMPI, Jerusalem, Israel) connected through a stimulus isolation unit to the concentric bipolar electrode. Field excitatory postsynaptic potentials (fEPSPs) evoked in layers II-III of the PRC by stimuli of increasing strength (20-220 µA) delivered at 0.033 Hz were recorded to obtain the input-output relations of the extracellular field potential. In LTP experiments, responses were recorded at 0.5-1.0 min intervals for 10 minutes before and for at least 60 min after theta burst stimulation (TBS). Stimulus intensity was adjusted to induce ~50% of the maximal synaptic response; after at least 10 min of stable baseline recording, TBS (four trains every 15 s, each train comprising 10 bursts of 5 pulses at 100 Hz, inter-burst interval 150 ms) was

applied to induce LTP. LTP was defined as an increase in fEPSP amplitude of at least 10% at 25-30 min after TBS, and for the remainder of the recording (60 min after TBS). Some slices were treated with the selective antagonists for GABA<sub>A</sub> receptors (picrotoxin, 100  $\mu$ M; Sigma-Aldrich) or GABA<sub>B</sub> receptors (CGP55845, 1  $\mu$ M; Sigma-Aldrich) during the whole recording session. All drugs applied were preliminarily dissolved in concentrated aliquots and stored at -20 °C, then re-dissolved to the final concentrations in artificial cerebrospinal fluid and delivered to the slice via general perfusion.

*Measurements.* The field excitatory postsynaptic potentials (fEPSPs) evoked in the PRC consisted of a negative going field potential, representing the excitatory synaptic response evoked by fibers distributed in the superficial layers. This potential was preceded by a negative-positive-negative fast wave, representing the compound action potential of the stimulated fibers (presynaptic volley). For reconstruction of the input-output relations, the amplitude of the presynaptic volley was measured from its initial positive peak to its negative peak, and the amplitude of the synaptic response was measured from the baseline to the maximum negativity. For the evaluation of LTP, the peak amplitude of the field potential was measured, and any change after TBS was expressed in relation to the normalized pre-conditioning baseline (mean of the fEPSP amplitudes recorded in the last 5 min before TBS).

### **RNA isolation and RT-qPCR**

RNA isolation and RT-qPCR were conducted on Cdk15 +/Y (n = 8) and Cdk15 -/Y (n = 8) mice. Animals were euthanized with isoflurane (2% in pure oxygen) and sacrificed through cervical dislocation. The brain was quickly removed, and the cortex underwent mRNA isolation using the TRI Reagent method according to the manufacturer's instructions (Sigma-Aldrich, St. Louis, MO, USA). cDNA synthesis was achieved with 2  $\mu$ g of total RNA using iScript™ Advanced cDNA Synthesis Kit (Bio-Rad, Hercules, CA, USA) according to the manufacturer's instructions. Real-time

PCR was performed using SsoAdvanced Universal SYBR Green Supermix (Bio-Rad) in an iQ5 Real-Time PCR Detection System (Bio-Rad). We used primer pairs (Supplementary table 1) that gave an efficiency close to 100%. Glyceraldehyde 3-phosphate dehydrogenase (GAPDH) was used as a reference gene for normalization in the qPCR. Relative quantification was performed using the  $\Delta\Delta C_t$  method (Livak and Schmittgen, 2001).

<b>Gene</b>	<b>Primer sequence (5'-3')</b>	
<b><i>GABA<sub>B</sub>R1b</i></b>	<i>Forward</i>	CTCTTCTGCTGGTGATGGC
	<i>Reverse</i>	TACTGCACGCCGTTCTGAG
<b><i>GABA<sub>B</sub>R2</i></b>	<i>Forward</i>	GACCTGCGACTCTACGACACC
	<i>Reverse</i>	GCGTTGTCTGAGGGCACC
<b><i>GABA<sub>A</sub>R1</i></b>	<i>Forward</i>	CCAAGTCTCCTTCTGGCTCAACA
	<i>Reverse</i>	GGGAGGGAATTTCTGGCACTGAT
<b><i>GABA<sub>A</sub>R2</i></b>	<i>Forward</i>	TTACAGTCCAAGCCGAATGTCCC
	<i>Reverse</i>	ACTTCTGAGGTTGTGTAAGCGTAGC
<b><i>GABA<sub>A</sub>R3</i></b>	<i>Forward</i>	CAAGAACCTGGGGACTTTGTGAA
	<i>Reverse</i>	AGCCGATCCAAGATTCTAGTGAA
<b><i>GABA<sub>A</sub>R4</i></b>	<i>Forward</i>	GAGACTGGTGGATTTTCCTATGG
	<i>Reverse</i>	GGTCCAGGTGTAGATCATCTCACT
<b><i>GABA<sub>A</sub>R5</i></b>	<i>Forward</i>	CCCTCCTTGTCTTCTGTATTTCC
	<i>Reverse</i>	TGATGTTGTCATTGGTCTCGTCT

**Table 1. List of primers used for quantitative RT-PCR.**

### **Histological analysis**

Histological analyses were conducted on behaviorally naïve animals (immunohistochemistry for VGAT and gephyrin) or vehicle/CGP55845- treated mice 1 h after behavioral testing (Golgi staining and immunohistochemistry for the scaffolding postsynaptic density protein 95, PSD95). Animals were euthanized with isoflurane (2% in pure oxygen) and sacrificed through cervical dislocation. Brains were quickly excised and cut along the midline. Right hemispheres were fixed by immersion in ice-cold 4% paraformaldehyde in 100mM phosphate buffer, pH 7.4, stored in fixative for 48 h, kept in 20% sucrose for an additional 24 h, and then frozen with cold ice.

Right hemispheres were cut using a freezing microtome into 30 µm-thick coronal sections which were serially collected in anti-freeze solution (30% glycerol; 30% ethylen-glycol; 10% PBS10X; 0.02% sodium azide; MilliQ to volume) and processed for immunohistochemistry procedures as described below. Left hemispheres were Golgi-stained as described below. All steps of sectioning, imaging, and data analysis were conducted blindly. For GABA<sub>B</sub>R immunofluorescence, animals were anesthetized with an intraperitoneal injection of Avertine (Sigma-Aldrich) and transcardially perfused, first with 10 mL 0.1 M PBS (pH 7.4) and then with ice-cold paraformaldehyde [4% in 0.1

M phosphate buffer (PB), pH 7.4]. After perfusion, the brains were dissected and kept in the same fixative solution overnight at 4°C. Brains were then cryoprotected by immersion in 10, 20, and 30% sucrose-PB solutions, cut in 30 µm sections with a cryostat and stored at -20°C in a solution containing 30% ethylene glycol and 25% glycerol until use.

### **Immunohistochemistry**

After several PBS rinses, one out of every 6 free-floating serial coronal sections of the PRC were put in a blocking solution for 1 h, followed by overnight incubation at room temperature with the following primary antibodies: rabbit polyclonal anti-VGAT antibody (1:500; Synaptic System), mouse monoclonal anti-gephyrin antibody (1:500; Synaptic System), rabbit polyclonal anti-PSD95 antibody (1:1000, Abcam), guinea pig polyclonal anti-GABABR antibody (1:2000; Chemicon). The following day, sections were washed and incubated with appropriate fluorescent secondary antibodies (1:200, Jackson ImmunoResearch Laboratories, Inc.). After several PBS rinses, the sections were mounted

on gelatin-coated glass slides and coverslipped with Dako fluorescence mounting medium (Dako Italia, Milan, Italy). For quantification of synaptic puncta, images that were processed for VGAT, gephyrin and PSD95 immunofluorescence were acquired with a Leica TCS SL confocal microscope. In each section, four images from the PRC were captured and the density of individual puncta exhibiting immunoreactivity for a specific antibody was evaluated in layers II-III, as previously described in (Pizzo et al., 2016). For the GABABR immunosignal analysis, confocal images of the PRC were acquired in corresponding sections from six animals per genotype with a laser scanning confocal microscope (LSM5 Pascal; Zeiss, Germany) using a 40× objective, 1 µm Z-step (1.4 numerical aperture) and the pinhole set at 1 Airy unit. Images were background subtracted with ImageJ software (NIH, USA) using the intensity of corpus callosum background staining as threshold. Immunopositive cells were manually counted using the point tool in ImageJ software (Image pro-

cessing and analysis in Java, NIH, USA). The ROI Manager tool in ImageJ software was employed to quantify integrated optical density.

### **Golgi staining**

Left hemispheres were Golgi-stained using the FD Rapid GolgiStain™ Kit (FD NeuroTechnologies, Columbia, MD, USA). Hemispheres were immersed in an impregnation solution which contained mercuric chloride, potassium dichromate, and potassium chromate and was stored at room temperature in the dark for 2–3 weeks. Hemispheres were cut using a microtome into 100 µm-thick coronal sections and then mounted on gelatin-coated glass slides and air dried at room temperature in the dark for an additional 2–3 days. After drying, sections were rinsed with distilled water and subsequently stained in the developing solution of the kit. A light microscope (Leica Microsystems) equipped with a motorized stage and focus control system and a color digital camera (Coolsnap-Pro; Media Cybernetics) were used to take bright field images. Measurements were carried out using Image Pro Plus software (Media Cybernetics).

***Spine density and morphology*** - In Golgi-stained sections, spines of apical dendritic branches of layer II-III perirhinal neurons were acquired using a 100X oil immersion objective lens. Dendritic spine density was measured by manually counting the number of dendritic spines. In each mouse, 12-15 dendritic segments (segment length: 10 µm) from each zone were analyzed and the density of the dendritic spines was expressed as the number of spines per 10 µm of dendrite. Based on their morphology, dendritic spines can be divided into two different categories, immature and mature. The number of spines belonging to each categories was counted and expressed as a percentage.

### **Western Blotting**

Western blot analyses were conducted on behaviorally naïve animals. Western blotting was carried out in homogenates of the PRC. which were obtained by cutting the brain into horizontal slices (400

µm-thick) taken during the same procedure used for the electrophysiological recording described above. PRC samples from four slices per animal gave a sufficient amount of material for western blot analysis. Total proteins were obtained as previously described (Trazzi et al., 2014). Protein concentration was determined using the Bradford method (Bradford, 1976). Equivalent amounts 50 µg of protein were subjected to electrophoresis on a BOLT Bis-Tris Plus gel (Thermo Fisher Scientific) and transferred to a Hybond ECL nitrocellulose membrane (Amersham - GE Healthcare Life Sciences). The following primary antibodies were used: rabbit polyclonal anti-VGAT antibody (1:1000; Synaptic System), mouse monoclonal anti-GABABR antibody (1:500; Merck Millipore), rabbit polyclonal anti-GIRK2 antibody (1:500; Alomone Labs), rabbit polyclonal anti-BDNF (1:500, Santa Cruz Biotechnology), and rabbit polyclonal anti-GAPDH (1:5000, Sigma-Aldrich). HRP-conjugated goat anti-rabbit or goat anti mouse IgG (1:5000, Jackson ImmunoResearch Laboratories) secondary antibody was used. Densitometric analysis of digitized images was performed using Chemidoc XRS Imaging Systems and Image Lab™ Software (Bio-Rad).

### **Behavioral Testing**

The animal behavioral test was performed by researchers who were blind to genotype and treatment. Mice were allowed to habituate to the testing room for at least 1 h before the test. The test was performed in an open-field arena (50x50 cm). The behavior of the mice was monitored using a video camera placed above the center of the arena. The experiments were scored using EthoVision XT ver. 14 software (Noldus). Test chambers were cleaned with 70% ethanol between test subjects.

***Pretraining Habituation*** -The animals were habituated in an empty (without objects) open-field arena for 2 days before the commencement of behavioral testing. Each animal was placed in the center of the arena and allowed to freely explore the open field for 20 min.

**Novel Object Preference Task** -The procedure involves a familiarization phase, followed by a preference test phase (Fig. 9A,B). In the familiarization phase a mouse is left for 10 minutes in the same arena (of the pretraining habituation), which in this phase contains 4 copies of the same object (a plastic tube too heavy to be moved by the mouse; objects 1-4), each of them placed near one of the four corners of the arena (15 cm from each adjacent wall). After an hour of interval, during which one of the 4 objects (object 1) is replaced by a new one (a wooden cube; objects 2-4 remain in the same position), the same mouse is placed again in the arena for the preference test phase (10 min duration; Fig. 9A,B). The exploration time is defined as the time in which the animal keeps the nose in the direction of the object at a distance of less than 2 cm (or touches it with the nose). The ability to discriminate between objects is calculated using the Exploratory Preference Index, i.e. the percentage of time spent exploring one of the 4 objects compared to the total time spent exploring the 4 objects (Wang et al., 2007); therefore a preference index above 25% indicates the preference for an object. For the study of the correlation between GABAergic inhibition and object recognition memory, the mice were treated (by intraperitoneal injection) before the beginning of the familiarization phase with the selective inhibitor of GABA<sub>B</sub> receptors CGP55845 (0.5 mg/kg in saline solution, 10 ml/kg) or with an equivalent volume of saline.

### **Statistical analysis**

If the data sets passed normality test and equal variance test, we performed Student's t-test or two-way ANOVA followed by Fischer or Tukey post hoc tests as specifically indicated in the text of each figure legend, using GraphPad Prism software (La Jolla). All values are presented as mean  $\pm$  SEM, and n indicates the number of mice. A probability level of  $p < 0.05$  was considered to be statistically significant.



## RESULTS

### GABAergic transmission in the perirhinal cortex of *Cdk15* $-/\gamma$ mice

An excess of inhibitory efficiency in the *Cdk15* KO mouse model was first suggested based on histological studies in the primary visual cortex, that demonstrated increased density of parvalbumin-positive inhibitory neurons and increased immunoreactivity of the vesicular GABA transporter VGAT, a protein selectively expressed in GABAergic axon terminals which can be taken as an index of the abundance of GABAergic inhibitory terminals (Lupori et al., 2019; Pizzo et al., 2016). To evaluate the balance between inhibitory and excitatory circuitry we stained for VGAT and we found an increased number of VGAT immunoreactive puncta (Fig. 1A,B). Similarly, VGAT levels were higher in homogenates of the PRC from *Cdk15*  $-/\gamma$  vs.  $+/\gamma$  mice (Fig. 2A,B).

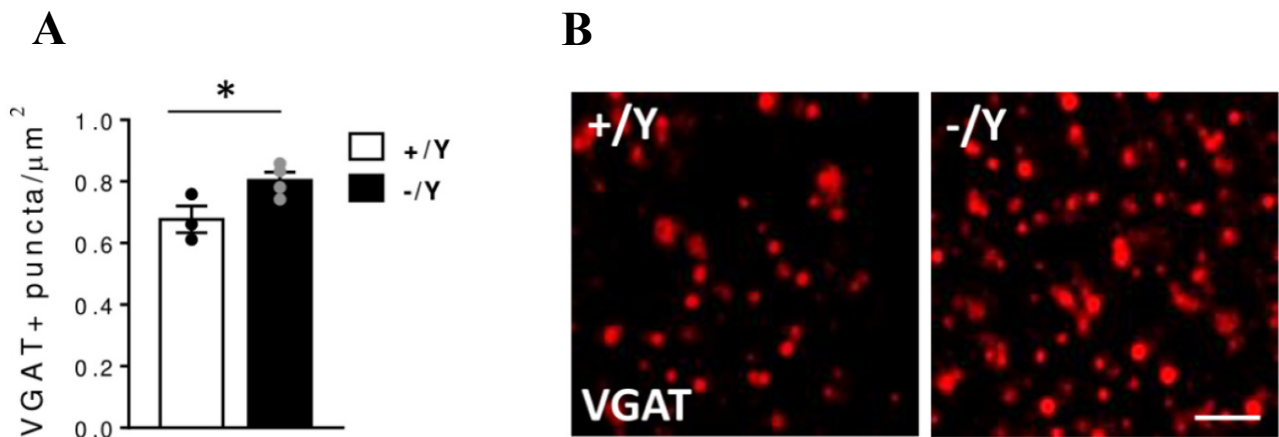


**Fig. 1.** (A) Number of VGAT positive puncta per  $\mu\text{m}^2$  in layer II-III of the PRC of  $+/\gamma$  ( $n = 3$  mice) and *Cdk15*  $-/\gamma$  ( $n = 4$  mice) mice. (B) Representative confocal images of PRC sections processed for VGAT immunohistochemistry from a *Cdk15*  $+/\gamma$  mouse and a *Cdk15*  $-/\gamma$  mouse. Scale bar = 2  $\mu\text{m}$ .

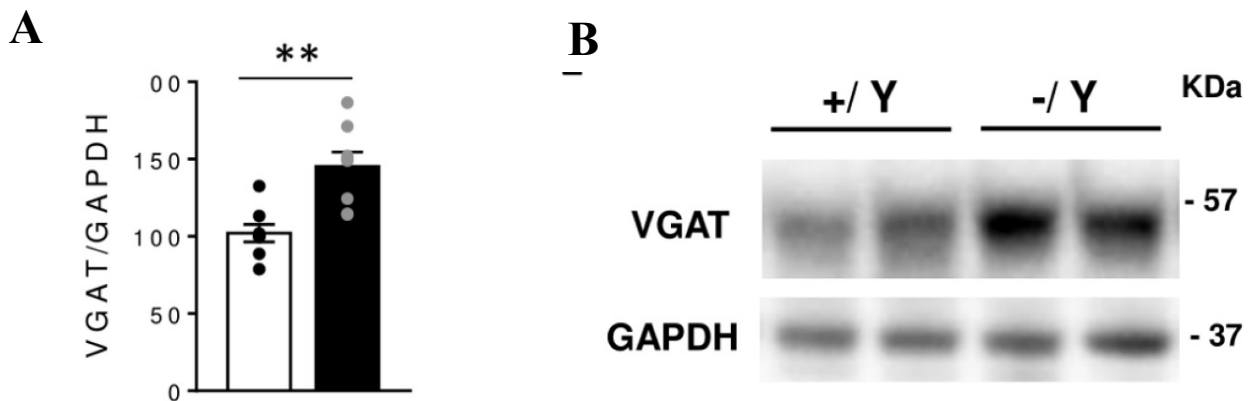


**Fig. 2.** (A) Western blot analysis of VGAT level normalized to glyceraldehyde 3-phosphatedehydrogenase (GAPDH) levels in PRC of *Cdk15* +/Y (n = 8 mice) and *Cdk15* -/Y (n = 8 mice) mice. (B) Immunoblots are examples of VGAT level in PRC extracts from 2 animals of each experimental group. Values represent mean  $\pm$  SEM. \*p < 0.05, \*\*\*p < 0.001 (Student's t-test).

Then we investigated the postsynaptic compartments starting from the expression of gephyrin, a scaffolding protein that anchors, clusters, and stabilizes GABA<sub>A</sub> receptors at inhibitory synapses (Choi and Ko, 2015). As shown in Fig. 3A and B, we found no significant changes in the density of gephyrin-positive puncta in the PRC of *Cdk15* -/Y mice.

The inhibitory signaling in the brain, including the PRC (Garden et al., 2002), is mainly mediated by GABA<sub>B</sub> receptors (GABA<sub>B</sub>Rs) (Terunuma et al., 2014) to both the presynaptic and postsynaptic sites of glutamatergic and GABAergic neurons. We evaluated the expression levels of the GABA<sub>B</sub>R in the PRC of *Cdk15* -/Y and +/Y mice using immunohistochemistry and western blot analysis. As shown in Fig. 4A-5C, no differences in the number of GABA<sub>B</sub>R1-positive cells (Fig. 4A,C), or in GABA<sub>B</sub>R1 expression levels (Fig. 5A,C) were observed. Interestingly, in the PRC we didn't find a difference in the levels of GIRK2, an inward rectifying K<sup>+</sup> channel activated by the GABA<sub>B</sub>R (Fig. 5B,C).

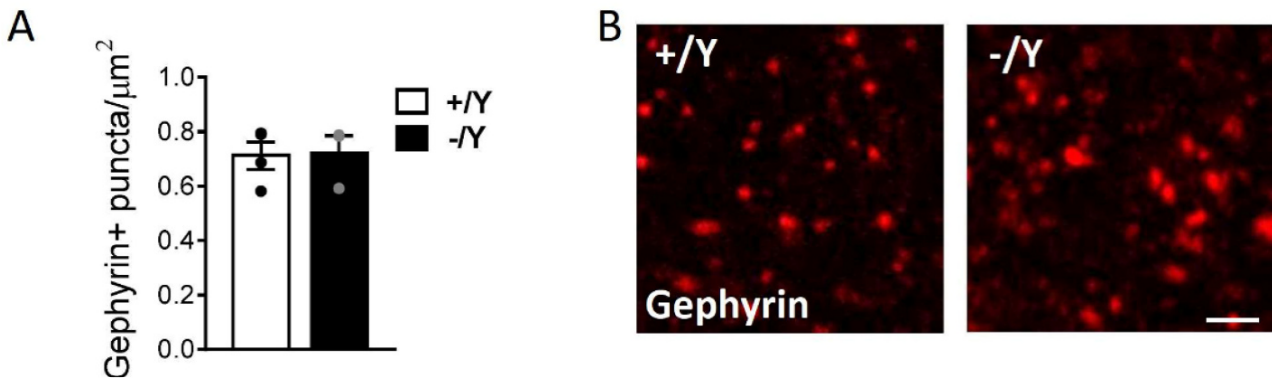


**Fig. 3.** (A) Number of gephyrin positive puncta per  $\mu\text{m}^2$  in layer II-III of the PRC of +/Y (n = 4 mice) and Cdk15 -/Y (n = 3 mice) mice. (B) Representative confocal images of PRC sections processed for gephyrin immunohistochemistry from a Cdk15 +/Y mouse and a Cdk15 -/Y mouse. Scale bar = 2  $\mu\text{m}$ .

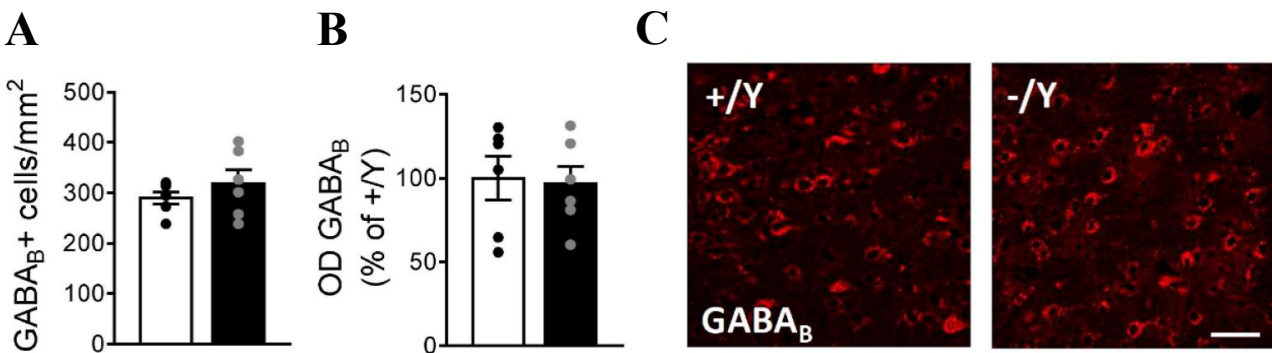


**Fig. 4.** (A) Number of GABA<sub>B</sub> positive cells per  $\text{mm}^2$  in layer II-III of the PRC of +/Y (n = 6 mice) and Cdk15 -/Y (n = 6 mice) mice. (B) Mean optical density (OD) of GABA<sub>B</sub> positive cells in the PRC of +/Y (n = 6 mice) and Cdk15 -/Y (n = 6 mice) mice expressed as % of the OD in Cdk15 +/Y mice. (C) Representative confocal images of PRC sections processed for GABA<sub>B</sub> immunohistochemistry from a Cdk15 +/Y mouse and a Cdk15 -/Y mouse. Scale bar = 25  $\mu\text{m}$ .

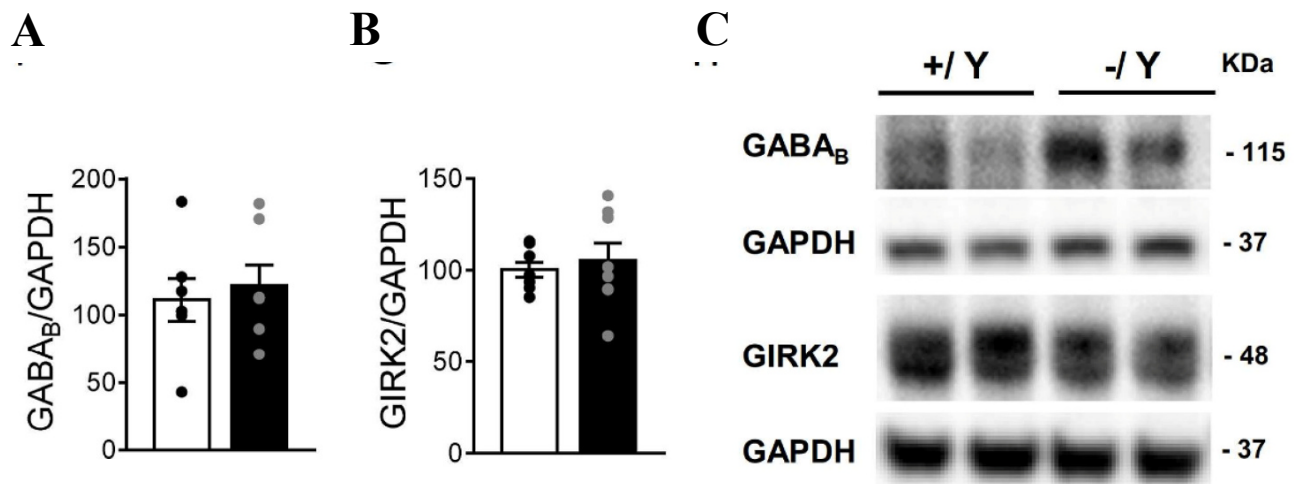
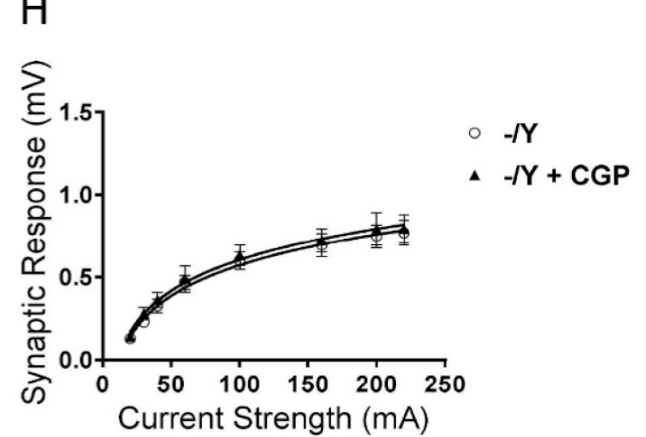
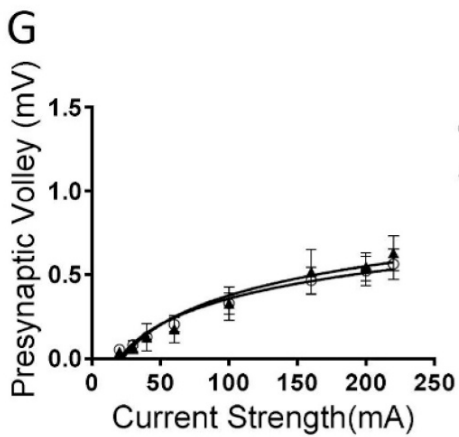
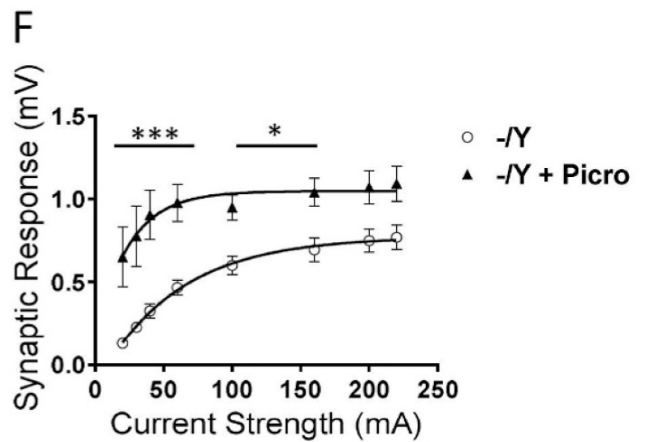
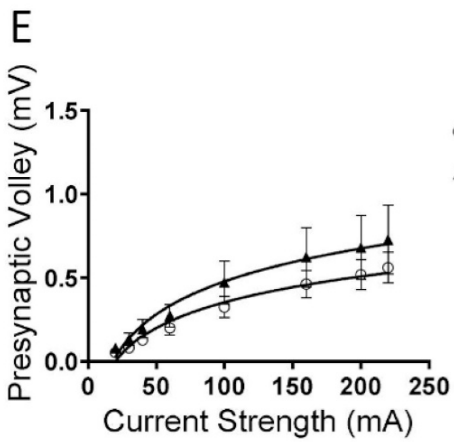
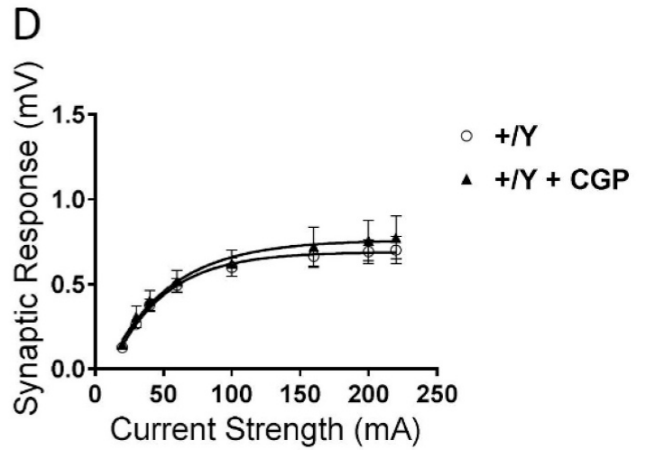
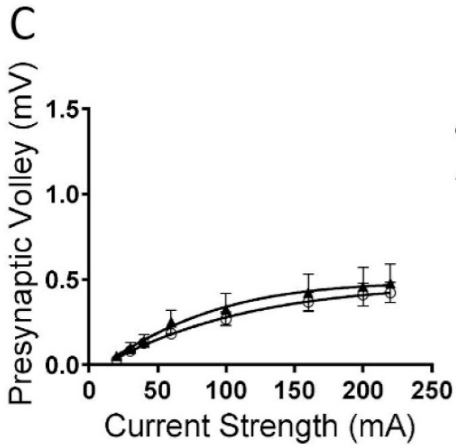
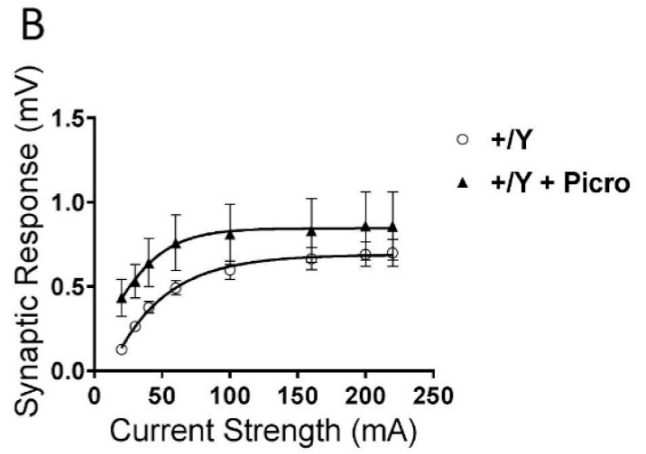
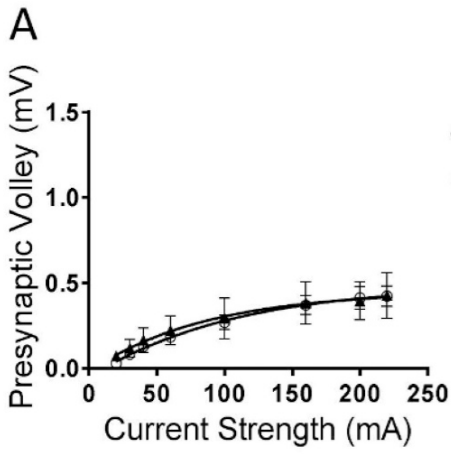


**Fig. 5.** (A) Western blot analysis of GABA<sub>B</sub>R1 levels normalized to GAPDH levels in the PRC of Cdk15 +/Y (n = 7 mice) and Cdk15 -/Y (n = 7 mice) mice. (B) Western blot analysis of GIRK2 levels normalized to GAPDH levels in the PRC of Cdk15 +/Y (n = 8 mice) and Cdk15 -/Y (n = 8 mice) mice. (C) Immunoblots are examples of GABA<sub>B</sub>R1, GIRK2 and GAPDH level in PRC extracts from 2 animals of each experimental group. Values represent mean ± SEM. (Student's t-test).

### Effect of GABA<sub>B</sub> and GABA<sub>A</sub> receptor antagonist on LTP in the perirhinal cortex in Cdk15 -/Y mice

To get further insight into the GABAergic inhibition through GABA<sub>A</sub> or GABA<sub>B</sub> receptors and to verify if it affects basal synaptic function, we examined the input-output relation in PRC slices after exposure of the slices to the GABA<sub>A</sub> receptor antagonist picrotoxin (100 μM), or the GABA<sub>B</sub> receptor antagonist CGP55845 (1 μM).

We found that in Cdk15 +/Y PRC slices exposed to picrotoxin or CGP55845 there was no increase in the magnitude of the afferent volley (Fig. 6A,C) or in that of the synaptic response (Fig. 6B,D). Similarly, in Cdk15 -/Y PRC slices exposed to picrotoxin or CGP55845 there was no increase in the magnitude of the afferent volley (Fig. 6E,G). Interestingly, we observed a significant increase in the magnitude of the synaptic response in Cdk15 -/Y PRC slices exposed to picrotoxin (Fig. 6F), but not to CGP55845 (Fig. 6H), suggesting that a GABAergic signaling inhibition, via GABA<sub>A</sub> receptors, induces an increase in the excitability of the Cdk15-deficient neurons in PRC.



---

**Fig. 6.** Effect picrotoxin and CGP55845 on input-output relations in the perirhinal cortex of *Cdkl5* +/Y and *Cdkl5* -/Y mice (A,B) Magnitude of presynaptic volley (A) and synaptic response (B) evoked in layers II/III PRC as a function of stimulus strength in control slices ( $n = 10$  slices from 8 mice) from *Cdkl5* +/Y mice and in picrotoxin (Picro; 100  $\mu$ M)-treated slices ( $n = 5$  slices from 4 mice) from *Cdkl5* +/Y mice. (C,D) Magnitude of presynaptic volley (C) and synaptic response (D) evoked in layers II/III PRC as a function of stimulus strength in control slices ( $n = 10$  slices from 8 mice) from *Cdkl5* +/Y mice and in CGP55845 (CGP; 1  $\mu$ M)-treated slices ( $n = 5$  slices from 4 mice) from *Cdkl5* +/Y mice. (E,F) Magnitude of presynaptic volley (E) and synaptic response (F) evoked in layers II/III PRC as a function of stimulus strength in control slices ( $n = 8$  slices from 8 mice) from *Cdkl5* -/Y mice and in picrotoxin-exposed slices ( $n = 5$  slices from 5 mice) from *Cdkl5* -/Y mice. (G,H) Magnitude of presynaptic volley (G) and synaptic response (H) evoked in layers II/III PRC as a function of stimulus strength in control slices ( $n = 8$  slices from 8 mice) from *Cdkl5* -/Y mice and CGP55845- exposed slices ( $n = 4$  slices from 3 mice) from *Cdkl5* -/Y mice. Values represent mean  $\pm$  SEM. \* $p < 0.05$ , \*\*\* $p < 0.001$  (Tukey's LSD after 2-WAY ANOVA).

***The GABA<sub>B</sub> receptor antagonist CGP55845 restored LTP magnitude in the perirhinal cortex of Cdkl5 -/Y mice***

LTP, induced by theta burst stimulation (TBS), has been shown to be reduced in the PRC of *Cdkl5* KO mice (Ren et al., 2019). In order to clarify whether excessive GABAergic inhibition might contribute to the LTP impairment, we carried out experiments in which PRC slices from *Cdkl5* -/Y or +/Y mice were pharmacologically disinhibited by picrotoxin (100  $\mu$ M), or CGP55845 (1  $\mu$ M). We found that in both *Cdkl5* -/Y and +/Y slices exposed to picrotoxin, the magnitude of LTP 55-60 min after TBS was lower in comparison with that of the corresponding untreated *Cdkl5* -/Y or +/Y slices (Fig. 7A,B). Fig. 8A,B show that in *Cdkl5* +/Y slices treated with the selective inhibitor of GABA<sub>B</sub> receptors, CGP5584775, the magnitude of LTP 55–60 min after TBS was similar to that of untreated *Cdkl5* +/Y. Importantly, LTP was restored in *Cdkl5* -/Y slices exposed to CGP55845 (Fig. 8A,B), suggesting that excessive inhibition mediated by GABA<sub>B</sub> receptors contributes to its impairment.

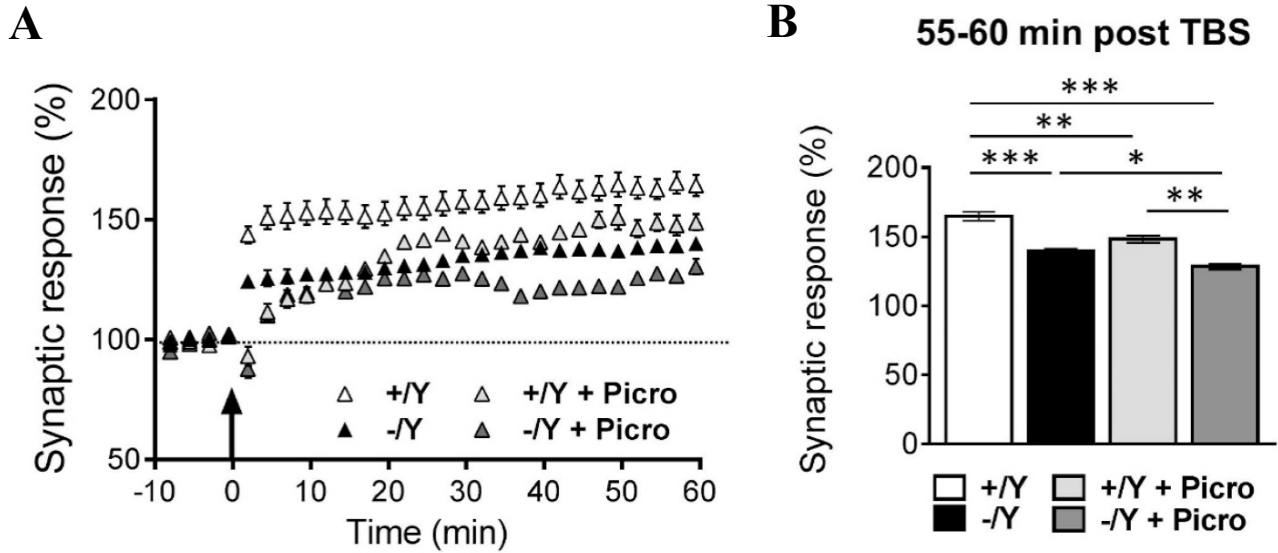


**Fig. 7.** Effect of picROTOXIN and CGP55845 on LTP in the perirhinal cortex of *Cdkl5* +/Y and *Cdkl5* -/Y mice (A) Magnitude of TBS-induced LTP in layers II-III PRC of *Cdkl5* +/Y and *Cdkl5* -/Y control slices and slices exposed to picROTOXIN (Picro; 100  $\mu$ M). Here and in the following panels (B–D), the magnitude of the response is expressed as a percentage of the average amplitude of responses recorded 10 min before LTP induction. Here, and in panel C, the arrow indicates the time of TBS delivery. Recordings were carried out in control slices ( $n = 9$  slices from 5 mice) from *Cdkl5* +/Y mice (+/Y), control slices ( $n = 11$  slices from 5 mice) from *Cdkl5* -/Y mice (-/Y), picROTOXIN-exposed slices ( $n = 5$  slices from 3 mice) from *Cdkl5* +/Y mice (+/Y + Picro), and picROTOXIN-exposed slices ( $n = 4$  slices from 3 mice) from *Cdkl5* -/Y mice (-/Y + Picro). (B) Averaged magnitude of the responses recorded 55–60 min after TBS (same data as in (A)).

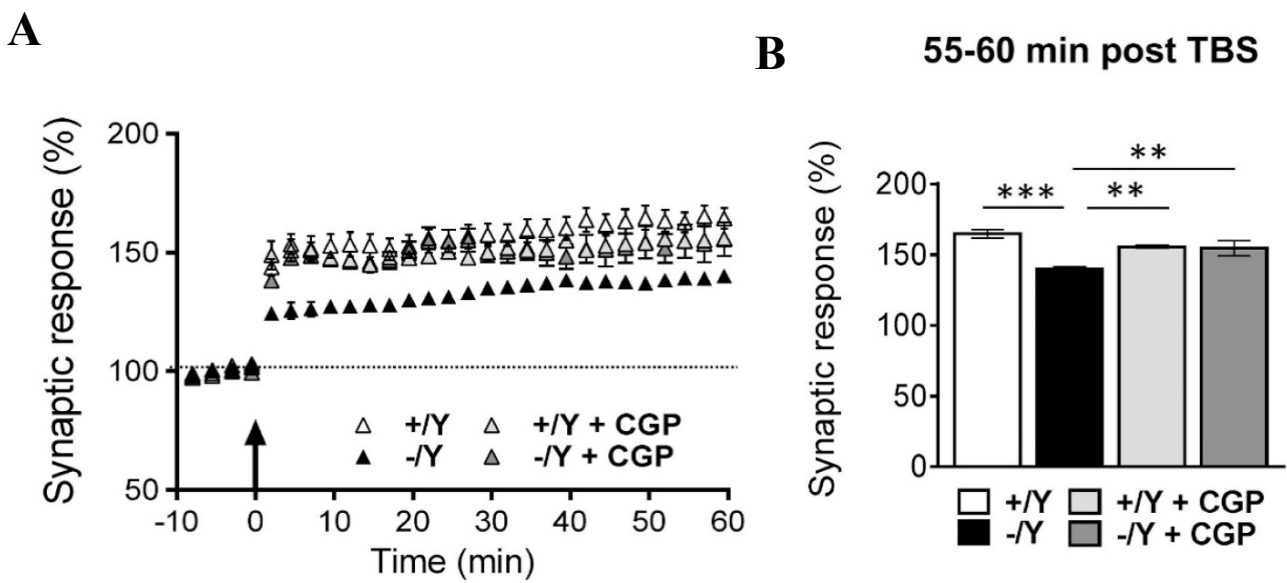


**Fig. 8.** (A) Magnitude of TBS-induced LTP in layers II-III PRC of *Cdkl5* +/Y and *Cdkl5* -/Y control slices and slices exposed to CGP55845 (CGP; 1  $\mu$ M). Recordings were carried out in control slices (n = 9 slices from 5 mice) from *Cdkl5* +/Y mice (+/Y), control slices (n = 11 slices from 5 mice) from *Cdkl5* -/Y mice (-/Y), CGP55845-exposed slices (n = 4 slices from 2 mice) from *Cdkl5* +/Y mice (+/Y + CGP) and CGP55845- exposed slices (n = 5 slices from 3 mice) from *Cdkl5* -/Y mice (-/Y + CGP). (B) Averaged magnitude of the responses recorded 55–60 min after TBS (same data reported in (C)). Values represent mean  $\pm$  SEM. \* $p$  < 0.05, \*\* $p$  < 0.01, \*\*\* $p$  < 0.001 (Tukey's LSD after 2-WAY ANOVA).

Recordings were carried out in control slices from 2-month-old *Cdkl5* +/Y (n=9) and *Cdkl5* -/Y (n=11) and slices from *Cdkl5* +/Y (n=5) and *Cdkl5* -/Y (n=4) exposed to CGP55845.

### **Altered novel object recognition memory in *Cdkl5* -/Y mice is rescued by treatment with the GABA<sub>B</sub> receptor antagonist CGP55845**

Balance between excitatory and inhibitory neurotransmission is a necessary pre-requisite for activity-dependent synaptic plasticity and, hence, efficient learning and memory. An important clinical feature in CDD is intellectual disability and, in particular, impairment of learning and memory. Studies of mouse genetic models have revealed that deficient visual recognition memory and spatial memory in CDD could be a result of reduced synaptic plasticity (Ren et al., 2019; Tang et al., 2017). NOR memory refers to the ability to judge a previously encountered item as familiar; in rodent brain, it depends on the integrity of the PRC (Bussey et al., 1999; Bussey et al., 2000). Interestingly, our research group recently reported that this kind of memory, evaluated using the NOR test, is impaired in *Cdkl5* -/Y mice (Ren et al., , 2019). As our electrophysiology data suggest that excessive activation of GABA<sub>B</sub> receptors contributes to LTP impairment in the PRC of *Cdkl5* -/Y mice, it is reasonable to hypothesize that it might also play a role in NOR memory impairment. To test this hypothesis, we investigated whether acute treatment with CGP555845 (0.5 mg/kg, i.p. injections 2 hours before NOR test; Fig. 9A) could improve NOR in *Cdkl5* KO mice.

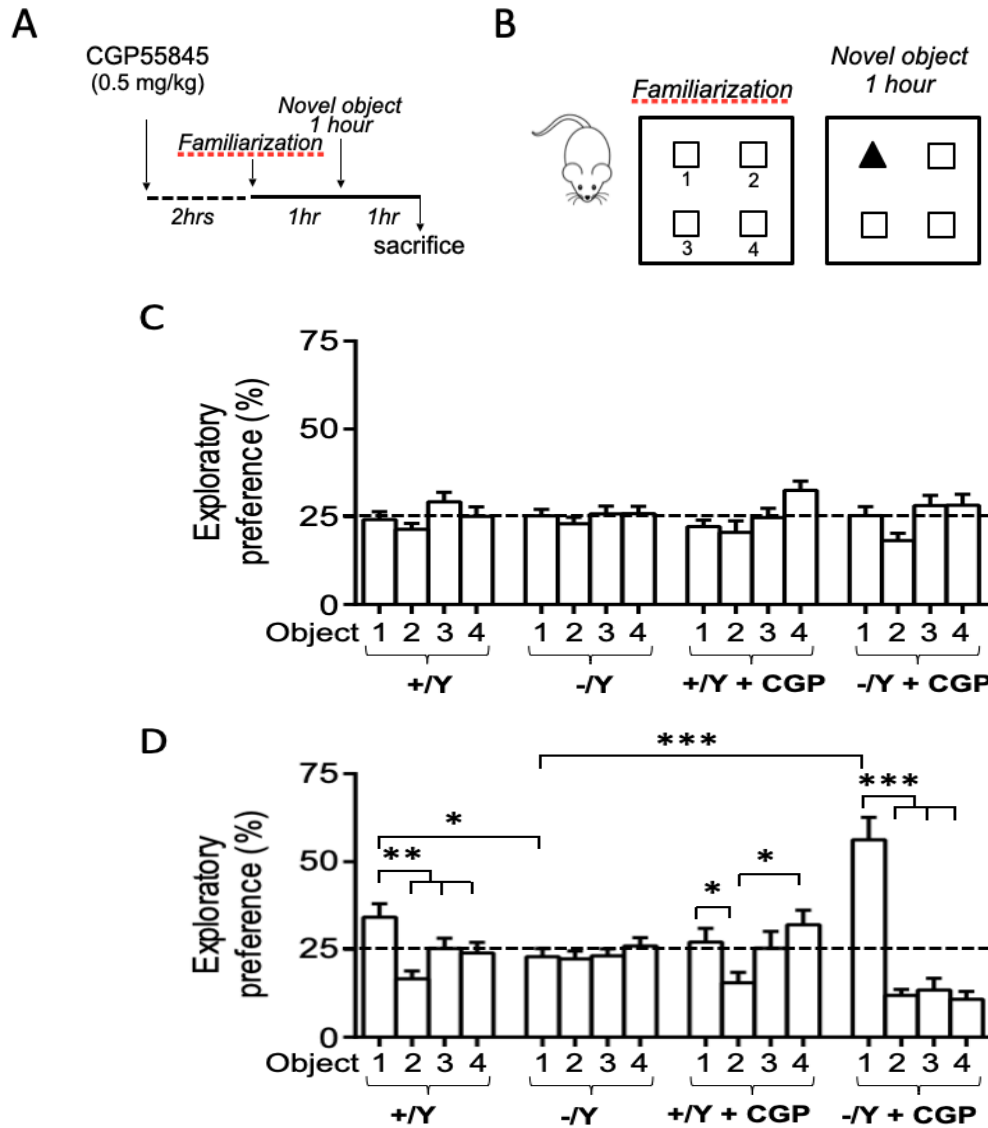


**Fig. 9.** Effect of treatment with CGP55845 on NOR memory in *Cdkl5* +/Y and *Cdkl5* -/Y mice (A,B) Experimental design for the NOR task. CGP55845 (0.5 mg/kg suspended in saline), or equivalent volume of saline only, was injected intraperitoneally in the mouse before the beginning of the familiarization phase, in which it was allowed to explore for 10 min four identical objects placed near the corners of a 50x50cm arena. After a delay of 1 h, during which one of the four objects (object 1) was replaced by a novel object, the animal was returned to the arena for the preference test phase (10 min duration). One hour later it was sacrificed for histological analyses. (C) Percentage of time spent exploring the four identical objects during the familiarization phase. Groups of mice: vehicle-treated *Cdkl5* +/Y (+/Y;  $n = 20$  mice), vehicle-treated *Cdkl5* -/Y (-/Y;  $n = 27$  mice), CGP55845-treated *Cdkl5* +/Y (+/Y + CGP;  $n = 14$  mice), CGP55845-treated *Cdkl5* -/Y (-/Y + CGP;  $n = 12$  mice) mice. (D) Percentage of time exploring the new object 1 and the previous identical objects 2–4 during the preference test phase (retention period of 1 h after familiarization). Same mice as in (C). Values represent mean  $\pm$  SEM. \* $p < 0.05$ , \*\* $p < 0.01$ , \*\*\* $p < 0.001$  (Fisher's LSD after 2-WAY ANOVA).

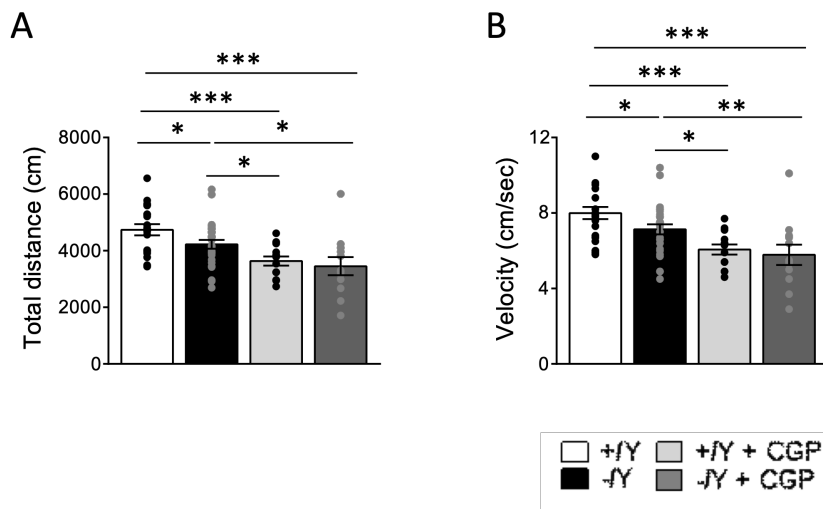


**Fig. 10.** Effects of treatment with CGP55845 on locomotor activity. Locomotor activity measured as total distance traveled (A) and average locomotion velocity (B) during the 10-min familiarization phase of the NOR test in vehicle-treated *Cdk15* +/Y (+/Y; n= 20 mice), vehicle-treated *Cdk15* -/Y (-/Y; n= 27 mice), CGP55845-treated *Cdk15* +/Y (+/Y + CGP; n= 13 mice), and CGP55845-treated *Cdk15* -/Y (-/Y + CGP; n= 12 mice) mice. Values represent mean  $\pm$  SEM. \* p < 0.05; \*\* p < 0.01; \*\*\* p < 0.001 (Fisher's LSD test after two-way ANOVA).

A 4-object NOR test was performed in an open-field arena, preceded by a 2-day habituation phase in the open field arena without objects (Fig. 9A,B). The NOR test started on the third day with a familiarization phase (10 min duration in the presence of 4 objects) followed, after a delay of 1 h (during which one of the four objects was replaced by a novel object), by the preference test phase (10 min duration). CGP55845 was injected 2 h before the familiarization phase (Fig. 9A,B).

In line with our previous results (Ren, 2019), while all groups of mice (+/Y n=20, -/Y n=27, +Y + CGP n=14, -/Y + CGP n=12) spent equal time exploring the four objects during the familiarization phase (Fig. 9C), in the test phase the preference index for the novel object in vehicle-treated *Cdk15* -/Y mice was significantly smaller than in vehicle-treated *Cdk15* +/Y mice (Fig. 9D), indicating a deficit in remembering the identity of an object in an open field. Interestingly, treatment with CGP55845 rescued NOR memory in *Cdk15* -/Y mice, whereas it impaired it in *Cdk15* +/Y mice

(Fig. 9D). These data suggests that an excess of GABA<sub>B</sub> inhibition could have a role in the deficit in NOR memory in CDD.

To monitor possible changes in spontaneous locomotion after treatment with CGP555845, the total distance traveled, and average velocity of movement were evaluated. *Cdkl5* <sup>-</sup>/<sub>Y</sub> mice showed a slightly reduced locomotor activity compared to *Cdkl5* <sup>+</sup>/<sub>Y</sub> mice (Fig 10 A). Interestingly, treatment with the GABA<sub>B</sub> receptor antagonist decreased spontaneous locomotor activity of both *Cdkl5* <sup>-</sup>/<sub>Y</sub> and <sup>+</sup>/<sub>Y</sub> mice (Fig 10 A,B). These observations suggest that the physiological balance between excitation and inhibition is crucial for motor behavior, and that the reduced locomotor activity observed in *Cdkl5* <sup>-</sup>/<sub>Y</sub> mice is not due to excessive GABA<sub>B</sub> receptor-mediated signaling.

### **Impaired spine number and maturation and synaptic connectivity in *Cdkl5* <sup>-</sup>/<sub>Y</sub> mice are improved by treatment with the GABA<sub>B</sub> receptor antagonist CGP55845**

We recently demonstrated that PRC neurons from *Cdkl5* mutant mice show several morphological alterations, including impaired spine density/maturation and impaired excitatory synaptic connectivity, as shown by a reduced number of PSD95 (postsynaptic density protein 95) - positive puncta (Ren et al., 2019). In order to evaluate whether the observed memory improvement induced by GABA<sub>B</sub> receptor inhibition is accompanied by a structural improvement, we measured spine density/maturation in Golgi-stained brain sections of vehicle-treated and CGP55845-treated mice. Mice vehicle-treated (<sup>+</sup>/<sub>Y</sub> n=4, <sup>-</sup>/<sub>Y</sub> n=4) and CGP55845-treated (<sup>+</sup>/<sub>Y</sub> + CGP n=4, <sup>-</sup>/<sub>Y</sub> +CGP n=5) were sacrificed 4 h after treatment. Treatment with CGP55845 significantly improved the number of spines (Fig. 11A,B), as well as the balance between immature and mature spines (Fig. 12A) in *Cdkl5* <sup>-</sup>/<sub>Y</sub> mice. Moreover, treatment with CGP55845 slightly, but significantly, increased the number of PSD95 immunoreactive puncta in the PRC of *Cdkl5* <sup>-</sup>/<sub>Y</sub> mice (Fig. 12B,C). On the contrary, treatment with CGP55845 had no effects on spine density (Fig. 10A) or maturation (Fig. 11B) in *Cdkl5* <sup>+</sup>/<sub>Y</sub> mice, while it significantly reduced the number of PSD95-positive puncta (Fig. 12B,C).

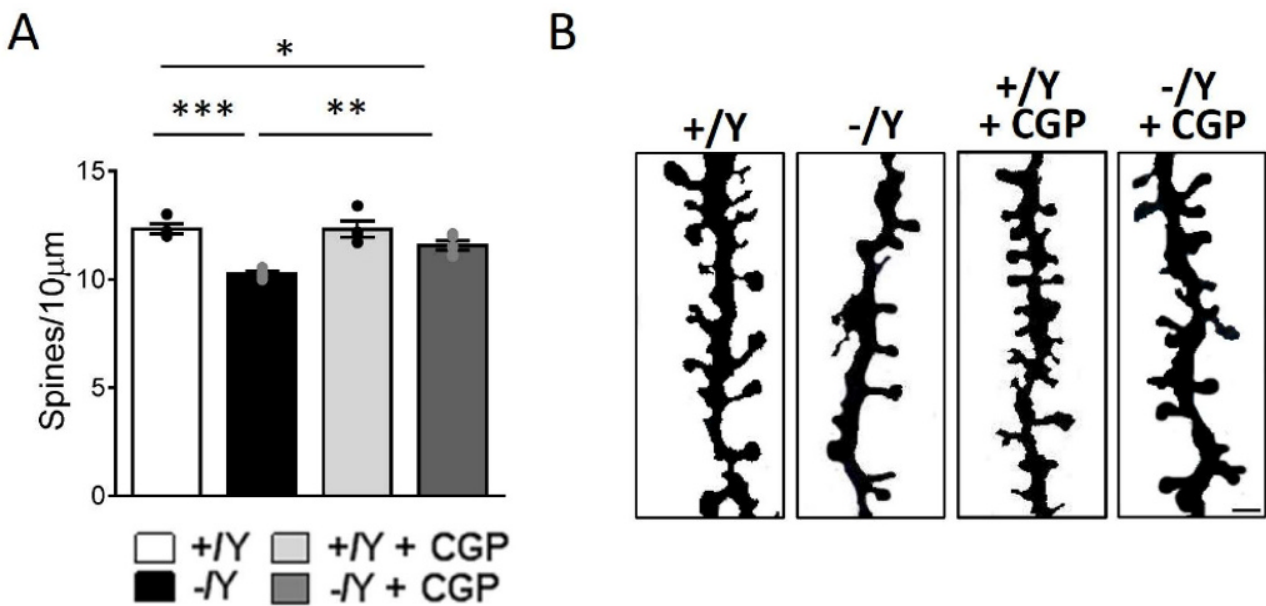


**Fig. 11.** Effects of treatment with CGP55845 on dendritic spines and synaptic connectivity in the perirhinal cortex of *Cdkl5* +/Y and *Cdkl5* -/Y mice (A) Dendritic spine density (number of spines per 10 µm) in apical dendrites of layer II-III PRC neurons of vehicle-treated (+/Y n = 4 mice; -/Y n = 4 mice) and CGP55845-treated (+/Y + CGP n = 4 mice; -/Y + CGP n = 5 mice) *Cdkl5* mice. (B) Examples of Golgi-stained apical dendritic branches of layer II-III PRC neurons of one animal from each experimental group. Scale bar = 1 µm.

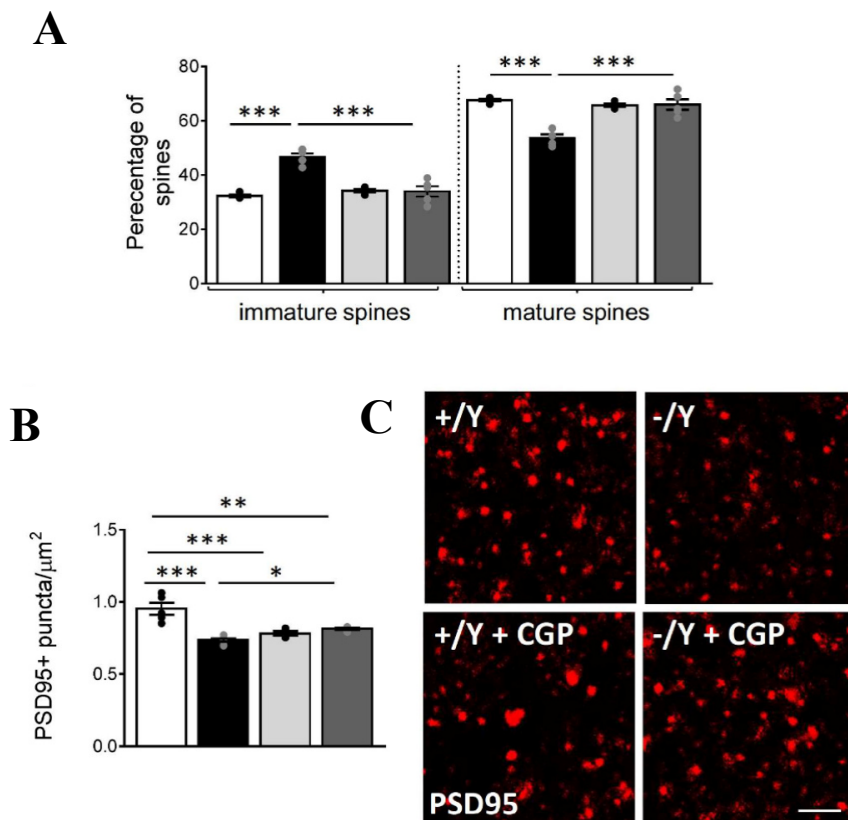


**Fig. 12.**(A) Percentage of immature (filopodia, thin, and stubby-shaped) and mature (mushroom- and cup-shaped) spines in relation to the total number of protrusions in layer II-III PRC neurons in mice as in (A). (B) Number of PSD95 positive puncta per  $\mu\text{m}^2$  in layer II-III of the PRC of vehicle-treated (+/Y n = 5 ce; -/Y n = 5 mice) and CGP55845-treated (+/Y + CGP n = 4 mice; -/Y + CGP n = 4 mice) *Cdk15* mice. (C) Confocal images of PRC sections processed for PSD95 immunohistochemistry of one animal from each experimental group. Scale bar = 2  $\mu\text{m}$ . Values represent mean  $\pm$  SEM. \*p < 0.05, \*\*p < 0.01, \*\*\*p < 0.001 (Fisher's LSD after 2-WAY ANOVA).

It was reported that GABA<sub>B</sub> antagonists increase brain levels of the brain-derived neurotrophic factor (BDNF) (Heese et al., 2000; Kleschevnikov et al., 2012), which is necessary for the formation and maturation of dendritic spines during postnatal development (Chapleau et al., 2009). To investi-

to investigate the molecular mechanisms underlying the improvement of dendritic spine maturation, we examined BDNF levels in PRC homogenates of *Cdk15*  $-/Y$  and  $+/Y$  mice following administration of vehicle or CGP55845. PRC samples were collected 2 h after treatment. Levels of BDNF were similar in *Cdk15*  $-/Y$  and *Cdk15*  $+/Y$  mice treated with the vehicle or CGP55845 (Fig. 13). Thus, the molecular mechanism underlying CGP55845-induced effects on dendritic spines remains to be determined.

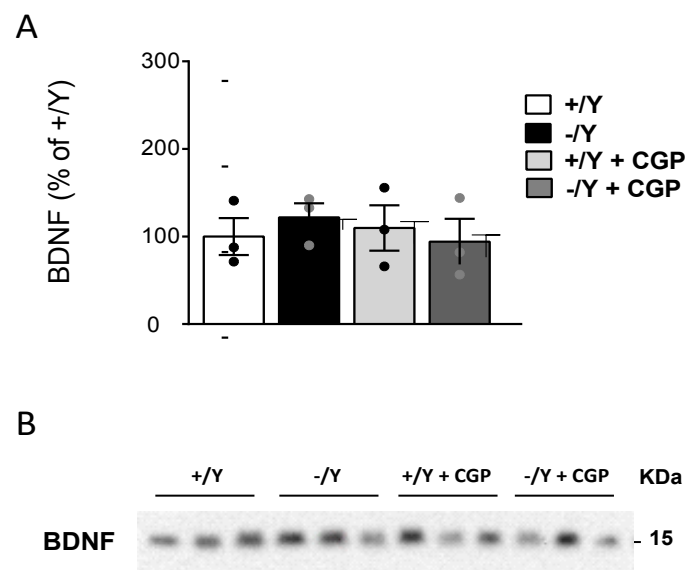


**Figura. 13.** Effects of treatment with CGP55845 on BDNF levels in the perirhinal cortex of *Cdk15*  $+/Y$  and *Cdk15*  $-/Y$  mice (A) Western blot analyses of BDNF levels in PRC homogenates of vehicle-treated ( $+/Y$   $n=3$  mice;  $-/Y$   $n=3$  mice) and CGP-treated ( $+/Y$   $n=3$  mice,  $-/Y$   $n=3$  mice) *Cdk15* mice. The intensity of immunostained bands was normalized against Ponceau stained total proteins. (B) Examples of immunoblots of PRC extracts from three animals of each experimental group. Values are expressed as percentage of vehicle-treated  $+/Y$  mice and are represented as means  $\pm$  SEM.

## DISCUSSION

CDD is an early-onset epileptic encephalopathy that shares common features with RTT, such as neurodevelopmental delay, stereotypic hand movements, hypotonia and impaired psychomotor development, and unique features like intractable epilepsy that is resistant to multiple antiepileptic drugs. CDD is a very severe pathology that strongly impairs the quality of life of patients and their families. No therapies are available at the moment.

A peculiar feature of the intellectual disability of these patients is an impairment of learning and memory. Studies in mice suggest that this deficit may be due to defects in neuronal maturation and synaptic plasticity (Ren et al., 2019; Tang et al., 2017), and disruption of the balance between excitation and inhibition (Della Sala et al., 2016; Pizzo et al., 2016; Ren et al., 2019).

In this study, we investigated the role of the GABAergic transmission in the PRC of Cdk15 KO mice and we found that an excessive GABAB-mediated inhibition contributes to LTP impairment in PRC slices, to visual recognition memory deficit and to alterations of dendritic spine morphology in PRC.

A previous study demonstrated an excess of inhibitory efficiency in the primary visual cortex of Cdk15 KO mice (Pizzo et al, 2016): they found an increased density of parvalbumin-positive inhibitory neurons and immunoreactivity of the vesicular GABA transporter (VGAT, a protein selectively expressed in GABAergic axon terminals). We found a similar increase in the levels of VGAT in PRC of the same mouse model. On the contrary, we found that the levels of gephyrin, GABAB receptors, GABAA receptors, and GIRK2 are not different in the PRC between Cdk15 KO and wild-type mice, suggesting that CDKL5 doesn't play a crucial role in the inhibitory post-synaptic compartment.

In electrophysiological experiments in PRC slices from Cdk15 <sup>-/-</sup> mice we focused on input-output relations of the excitatory transmission mediated by glutamate, and how it could be affected by in-

hibition of GABAA and GABAB receptors. We found that the magnitude of the synaptic response was significantly increased by GABAA receptor inhibition, whereas the afferent volley remained unchanged. It means that the exposure to picrotoxin, which blocks the GABAA receptors, increases the excitation of PRC glutamatergic neurons without affecting the excitability of the neurons whose fibers activate them. The increase of excitation might depend on a stronger excitatory input that is needed to compensate the increased efficiency of GABAergic inhibition (increased number of VGAT-positive pre-synaptic terminals) and is unmasked when GABAA receptors are blocked by picrotoxin. Accordingly, picrotoxin had no effect on input-output relation of glutamatergic synaptic transmission in the PRC of Cdk15 +/Y mice, where the balance between inhibition and excitation is physiological. The observation that inhibition of GABAB receptors had no effect on the magnitude of the afferent volley or synaptic response in both Cdk15 -/Y and +/Y mice is not surprising, as they are coupled to G proteins and influence synaptic transmission over a slower timescale.

The LTP induced by TBS has previously been shown to be reduced in the PRC of Cdk15 KO mice (Ren, 2019). Interestingly, here we found that exposure to CGP55845 restored LTP magnitude in Cdk15 -/Y PRC slices, suggesting that excessive inhibition mediated by GABAB receptors contributes to its impairment. GABA can interact at both GABAB autoreceptors as well as at presynaptic and postsynaptic GABAB heteroreceptors in glutamatergic neurons (Gassmann and Bettler, 2012). The effect of GABAB receptor blockade on LTP suggests that the abnormality of the GABAergic system in the PRC of Cdk15 -/Y mice may include an imbalance towards a greater number of heteroreceptors on glutamatergic neurons. The mechanism underlying CGP55845-induced LTP restoration may include increase of glutamate release due to presynaptic GABAB receptor blockade, and increase of Ca<sup>2+</sup> entry through NMDA glutamate receptors due to postsynaptic GABAB receptor blockade (Chalifoux and Carter, 2010; Morrisett et al., 1991). In line with this hypothesis and with a previous observation (Roncace et al., 2017), exposure to CGP55845 did not

change the magnitude of LTP in the PRC of wild-type mice, where the balance between GABAB heteroreceptors and autoreceptors is physiological.

Exposure to the GABAA receptor blocker picrotoxin decreased LTP magnitude in the PRC in both wild-type ((Roncace et al., 2017) and present findings) and  $-/Y$  mice. This might be caused by disinhibition (i. e. blockade of GABAA-mediated inhibition) of inhibitory interneurons that act on glutamatergic neurons through GABAB receptors. This hypothesis takes into account the apparent discrepancy that picrotoxin increased synaptic response only in  $-/Y$  mice, whereas it decreased LTP in both  $-/Y$  and  $+/Y$  mice. Being based on inhibition mediated by GABAB receptors, the above reported disinhibition can only be effective on synaptic plasticity, due to the slow timescale of its effects.

Interestingly, we found that impaired PRC-dependent NOR memory is rescued by acute treatment with the GABAB receptor antagonist CGP55845. This finding is fully in line with our evidence showing that treatment with CGP55845 restored LTP and increased the number of PSD95 positive puncta as well as the number and maturation of dendritic spines in  $Cdk15$   $-/Y$  mice PRC. The structural changes observed just 4 h after treatment with CGP55845 in the dendrites are consistent with those observed within an hour during LTP in vitro (Engert and Bonhoeffer, 1999; Toni et al., 1999), and in the living brain during learning (Xu et al., 2009). Moreover, it has been shown that PSD-95 accumulation in spines occurs within a few minutes to hours after initial contact between the nascent spine and a presynaptic partner in neuronal cultures (Bresler et al., 2001; Friedman et al., 2000; Okabe et al., 2001).

Besides these improvements, it is reasonable to suppose that additional effects occurring in PRC and in other brain regions may contribute to the effect on memory of GABAB receptor inhibition. In contrast to the effects observed in  $Cdk15$  KO mice, memory performance of wild-type mice worsened and the density of PSD95 positive synaptic puncta decreased after CGP55845 administration. Although not in agreement with a previous observation (Kleschevnikov et al., 2012), this result is

not surprising, as the performance of wild-type mice is based on the physiological balance between excitation and inhibition. Indeed, our results indicate that alterations of this balance, resulting from either increase or decrease of GABAB receptor-mediated inhibition, lead to deterioration of memory performance.

Taken together, present findings suggest that inhibition of excessive GABAB receptor-mediated signaling efficiently improves synaptic plasticity and memory in a mouse model of CDKL5 deficiency.

## REFERENCES

- Amendola E, Zhan Y, Mattucci C, Castroflorio E, Calcagno E, Fuchs C, Lonetti G, Silingardi D, Vyssotski AL, Farley D, Ciani E, Pizzorusso T, Giustetto M, Gross CT (2014) Mapping pathological phenotypes in a mouse model of CDKL5 disorder. *PLoS One* 9:e91613.
- Bahi-Buisson N, Nectoux J, Rosas-Vargas H, Milh M, Boddaert N, Girard B, Cances C, Ville D, Afenjar A, Rio M, Heron D, N'Guyen Morel MA, Arzimanoglou A, Philippe C, Jonveaux P, Chelly J, Bienvenu T (2008b) Key clinical features to identify girls with CDKL5 mutations. *Brain : a journal of neurology* 131:2647-2661.
- Brown, M.W., Aggleton, J.P. (2001). Recognition memory: what are the roles of the perirhinal cortex and hippocampus? *Nat. Rev. Neurosci.* 2, 51–61.
- Bussey T J, Muir J L. Aggleton (1999). Functionally dissociating aspects of event memory: the effects of combined perirhinal and postrhinal cortex lesions on object and place memory in the rat . *J Neurosci.* 19(1):495-502
- Bussey T J, Duck J, Muir J L, Aggleton J P (2000). Distinct patterns of behavioural impairments resulting from fornix transection or neurotoxic lesions of the perirhinal and postrhinal cortices in the rat. *Behave Brain Res.* 111(1-2):187.202.
- Chen Q, Zhu YC, Yu J, Miao S, Zheng J, Xu L, Zhou Y, Li D, Zhang C, Tao J, Xiong ZQ (2010) CDKL5, a protein associated with rett syndrome, regulates neuronal morphogenesis via Rac1 signaling. *J Neurosci* 30:12777-12786.
- Chooi, G., Ko, J. (2015) Gephyrin: a central GABAergic synapse organizer. *Exp. Mol. Med.* 47, e158.

- Della Sala G, Putignano E, Chelini G, Melani R, Calcagno E, Michele Ratto G, Amendola E, Gross CT, Giustetto M, Pizzorusso T (2016) Dendritic Spine Instability in a Mouse Model of CDKL5 Disorder Is Rescued by Insulin-like Growth Factor 1. *Biol Psychiatry* 80:302-311
- Fehr S, Wilson M, Downs J, Williams S, Murgia A, Sartori S, Vecchi M, Ho G, Polli R, Psoni S, Bao X, de Klerk N, Leonard H, Christodoulou J (2013) The CDKL5 disorder is an independent clinical entity associated with early-onset encephalopathy. *Eur J Hum Genet* 21:266-273.
- Fehr S, Wong K, Chin R, Williams S, de Klerk N, Forbes D, Krishnaraj R, Christodoulou J, Downs J, Leonard H (2016) Seizure variables and their relationship to genotype and functional abilities in the CDKL5 disorder. *Neurology* 87:2206-2213.
- Fuchs C, Rimondini R, Viggiano R, Trazzi S, De Franceschi M, Bartesaghi R, Ciani E (2015) Inhibition of GSK3beta rescues hippocampal development and learning in a mouse model of CDKL5 disorder. *Neurobiol Dis* 82:298-310.
- Fuchs C, Trazzi S, Roberta T, Viggiano R, De Franceschi M, E. A, Gross CT, Calzà L, Bartesaghi R, Ciani E (2014a) Loss of Cdkl5 impairs survival and dendritic growth of newborn neurons by altering AKT/GSK-3beta signaling. *Neurobiology of disease* doi: 10.1016/j.nbd.2014.06.006.
- Garden, D.L., et al. (2002) Differences in GABAergic transmission between two inputs into the perirhinal cortex. *Eur. J. Neurosci.* 16, 437–444.
- Gennaccaro L, Fuchs C, Loi M, Roncacè V, Trazzi S, Ait-Bali Y, Galvani G, Berardi A C, Medici G, Tassinari M, Ren E, Rimondini R, Giustetto M, Aicardi G, Ciani E (2021) A GABAB receptor antagonist rescues functional and structural impairments in the perirhinal cortex of a mouse model of CDKL5 deficiency disorder. *Neurobiol Dis*, 153, 105304
- Guerrini R, Parrini E (2012) Epilepsy in Rett syndrome, and CDKL5- and FOXP1-related encephalopathies. *Epilepsia* 53:2067-2078.

- Kalscheuer VM, Tao J, Donnelly A, Hollway G, Schwinger E, Kubart S, Menzel C, Hoeltzenbein M, Tommerup N, Eyre H, Harbord M, Haan E, Sutherland GR, Ropers HH, Geetz J (2003) Disruption of the serine/threonine kinase 9 gene causes severe X-linked infantile spasms and mental retardation. *American journal of human genetics* 72:1401-1411.
- Kilstrup-Nielsen C, Rusconi L, La Montanara P, Ciceri D, Bergo A, Bedogni F, Landsberger N (2012) What we know and would like to know about CDKL5 and its involvement in epileptic encephalopathy. *Neural Plast* 2012:728267
- Alexander M, Kleschevnikov, Pavel V, Belichenko, Mehrdad Faizi, Lucia F. Jacobs, Khin Htun, Mehrdad Shamloo, and William C. Mobley (2012) Deficits in Cognition and Synaptic Plasticity in a Mouse Model of Down Syndrome Ameliorated by GABAB Receptor Antagonists. *The Journal of Neuroscience*, 32(27):9217–9227.
- Lin C, Franco B, Rosner MR (2005) CDKL5/Stk9 kinase inactivation is associated with neuronal developmental disorders. *Hum Mol Genet* 14:3775-3786.
- Mari F, Azimonti S, Bertani I, Bolognese F, Colombo E, Caselli R, Scala E, Longo I, Grosso S, Pescucci C, Ariani F, Hayek G, Balestri P, Bergo A, Badaracco G, Zappella M, Broccoli V, Renieri A, Kilstrup -Nielsen C, Landsberger N (2005) CDKL5 belongs to the same molecular pathway of MeCP2 and it is responsible for the early-onset seizure variant of Rett syndrome. *Hum Mol Genet* 14:1935-1946.
- Montini E, Andolfi G, Caruso A, Buchner G, Walpole SM, Mariani M, Consalez G, Trump D, Ballabio A, Franco B (1998) Identification and characterization of a novel serine-threonine kinase gene from the Xp22 region. *Genomics* 51:427-433.
- Nawaz MS, Giarda E, Bedogni F, La Montanara P, Ricciardi S, Ciceri D, Alberio T, Landsberger N, Rusconi L, Kilstrup-Nielsen C (2016) CDKL5 and Shootin1 Interact and Concur in Regulating Neuronal Polarization. *PLoS One* 11:e0148634

- Okuda K, Kobayashi S, Fukaya M, Watanabe A, Murakami T, Hagiwara M, Sato T, Ueno H, Ogonuki N, Komano-Inoue S, Manabe H, Yamaguchi M, Ogura A, Asahara H, Sakagami H, Mizuguchi M, Manabe T, Tanaka T (2017) CDKL5 controls postsynaptic localization of GluN2B-containing NMDA receptors in the hippocampus and regulates seizure susceptibility. *Neurobiol Dis* 106:158-170.
- Pizzo R, Gurgone A, Castroflorio E, Amendola E, Gross C, Sassoe -Pognetto M, Giustetto M (2016) Lack of Cdkl5 Disrupts the Organization of Excitatory and Inhibitory Synapses and Parvalbumin Interneurons in the Primary Visual Cortex. *Front Cell Neurosci* 10:261.
- Purpura DP (1974) Dendritic spine "dysgenesis" and mental retardation. *Science* 186:1126-1128.
- Ricciardi S, Ungaro F, Hambrock M, Rademacher N, Stefanelli G, Brambilla D, Sessa A, Magagnotti C, Bachi A, Giarda E, Verpelli C, Kilstrup-Nielsen C, Sala C, Kalscheuer VM, Broccoli V (2012) CDKL5 ensures excitatory synapse stability by reinforcing NGL-1-PSD95 interaction in the postsynaptic compartment and is impaired in patient iPSC-derived neurons. *Nat Cell Biol* 14:911-923.
- Rusconi L, Kilstrup-Nielsen C, Landsberger N (2011) Extrasynaptic N-methyl-D-aspartate (NMDA) receptor stimulation induces cytoplasmic translocation of the CDKL5 kinase and its proteasomal degradation. *J Biol Chem* 286:36550-36558.
- Rusconi L, Salvatoni L, Giudici L, Bertani I, Kilstrup-Nielsen C, Broccoli V, Landsberger N (2008) CDKL5 expression is modulated during neuronal development and its subcellular distribution is tightly regulated by the C-terminal tail. *J Biol Chem* 283:30101-30111.
- Tang S, Wang IJ, Yue C, Takano H, Terzic B, Pance K, Lee JY, Cui Y, Coulter DA, Zhou Z (2017) Loss of CDKL5 in Glutamatergic Neurons Disrupts Hippocampal Microcircuitry and Leads to Memory Impairment in Mice. *J Neurosci* 37:7420-7437.

- Terunuma, M, et al. (2014). Postsynaptic GABAB receptor activity regulates excitatory neuronal architecture and spatial memory. *J. Neurosci.* 34, 804–816.
- Tolia Kimberley F., Jay B. Bikoff, Christina G. Kane, Christos S. Tolia, Linda Hu, and Michael E. Greenberg (2007) The Rac1 guanine nucleotide exchange factor Tiam1 mediates EphB receptor-dependent dendritic spine development *PNAS* 17:7265-7270.
- Trazzi S, De Franceschi M, Fuchs C, Bastianini S, Viggiano R, Lupori L, Mazziotti R, Medici G, Lo Martire V, Ren E, Rimondini R, Zoccoli G, Bartesaghi R, Pizzorusso T, Ciani E (2018) CDKL5 protein substitution therapy rescues neurological phenotypes of a mouse model of CDKL5 disorder. *Hum Mol Genet* 27:1572-1592.
- Trazzi S, Fuchs C, Viggiano R, De Franceschi M, Valli E, Jedynek P, Hansen FK, Perini G, Rimondini R, Kurz T, Bartesaghi R, Ciani E (2016) HDAC4: a key factor underlying brain developmental alterations in CDKL5 disorder. *Hum Mol Genet* 25:3887-3907
- Valli E, Trazzi S, Fuchs C, Erriquez D, Bartesaghi R, Perini G, Ciani E (2012) CDKL5, a novel MYCN -repressed gene, blocks cell cycle and promotes differentiation of neuronal cells. *Biochim Biophys Acta* 1819:1173-1185.
- Wang Y, Wang W, Li D, Li M, Wang P, Wen J, Liang M, Su B, Yin Y (2014) IGF-1 alleviates NMDA-induced excitotoxicity in cultured hippocampal neurons against autophagy via the NR2B/PI3K-AKT-mTOR pathway. *J Cell Physiol* 229:1618-1629.
- Weaving LS, Christodoulou J, Williamson SL, Friend KL, McKenzie OL, Archer H, Evans J, Clarke A, Pelka GJ, Tam PP, Watson C, Lahooti H, Ellaway CJ, Bennetts B, Leonard H, Gecz J (2004) Mutations of CDKL5 cause a severe neurodevelopmental disorder with infantile spasms and mental retardation. *American journal of human genetics* 75:1079-1093.
- Zhong Xie, Deepak P. Srivastava , Huzefa Photowala, Li Kai, Michael E. Cahill, Kevin M Woolfrey, Cassandra Y. Shum, D. James Surmeier, and Peter Penzes (2007) Kalirin-7 controls activity-dependent structural and functiona plasticity of dendritic spines. *NIH* 56(4): 640–656.

- Zhou A, Han S, Zhou ZJ (2017) Molecular and genetic insights into an infantile epileptic encephalopathy - CDKL5 disorder. *Front Biol (Beijing)* 12:1-6.
- Zhu YC, Li D, Wang L, Lu B, Zheng J, Zhao SL, Zeng R, Xiong ZQ (2013) Palmitoylation -dependent CDKL5-PSD- 95 interaction regulates synaptic targeting of CDKL5 and dendritic spine development. *Proc Natl Acad Sci U S A* 110:9118-9123.
- Ziakopoulos Z, Brown MW, Bashir ZI. (2000) GABAB receptors mediate frequency-dependent depression of excitatory potentials in rat perirhinal cortex in vitro. *Eur J Neurosci.*12(3):803-9

